Role of oxidized phospholipids in inflammatory pain

Rolle von oxidierten Phospholipiden bei entzündlichen Schmerzen

Doctoral thesis for a doctoral degree

At the Graduate School of Life Sciences,

Julius-Maximilians-Universität Würzburg,

Section Neuroscience and Clinical

Submitted by

Milad Mohammadi

From

Tehran

Würzburg 2019

Submitted on: ……..……..

Office stamp

Members of the *Promotionskomitee*:

Chairperson: Prof. Dr. Paul Pauli

Primary Supervisor: Prof. Dr. Heike Rittner

Supervisor (Second): PD Dr. Robert Blum

Supervisor (Third): Prof. Dr. Nurcan Üçeyler

Supervisor (Fourth): Dr. Beatrice Oehler

Date of Public Defence: ……..……

Date of Receipt of Certificates: …….

List of abbreviations

4-HNE	4-hydroxynonenal
5-LO	5-lipoxygenase
Ab	antibody
AITC	allyl isothiocyanate
ANOVA	analysis of variance
ApoA-I	apolipoprotein A-I
BSA	bovine serum albumin
CFA	complete Freund's adjuvant
DAMP	damage-associated molecular patterns
DAPI	4', 6-diamidino-2-phenylindole
DMSO	dimethyl sulfoxide
DRG	dorsal root ganglia
EDTA	ethylenediaminetetraacetic acid
FI	fluorescence intensity
HEK	human embryonic kidney
IASP	international association of study of pain
IF	immunofluorescence
KO	knockout
LPS	lipopolysaccharide
mAb	monoclonal antibody
NSAID	nonsteroidal anti-inflammatory drugs
ON	over night
OSE	oxidation-specific epitopes
OxLDL	oxidized low density lipoprotein
OxPAPC	oxidized 1-palmitoyl-2-arachidonoyl-sn-glycero-3-phosphocholine
OxPL	oxidized phospholipids
pAb	polyclonal antibody
PBS	phosphate buffered saline
PC	phosphatidylcholine
PEIPC	1-palmitoyl-2-(5,6)-epoxyisoprostaneE_2-*sn*-glycero-3-phosphocholine
PFA	paraformaldehyde
PGPC	1-palmitoyl-2-glutaryl-*sn*-glycero-3-phosphocholine
POVPC	1-palmitoyl-2-(5-oxovaleroyl)-*sn*-glycero-3-phosphocholine

PPT	paw pressure threshold
PRR	pattern recognition receptors
PWL	paw withdrawal latency
RM	repeated measures
RNS	reactive nitrogen species
ROS	reactive oxygen species
RT	room temperature
SEM	standard error of the mean
SP	substance P
TLR	toll like receptor
TRPA1	transient receptor potential ankyrin 1
TRPV1	transient receptor potential vanilloid 1
VF	von Frey
VGSC	voltage-gated sodium channels
WT	wild type

Table of contents

Summary

Introduction: During inflammation, reactive oxygen species (ROS) such as Hydrogen peroxide accumulate at the inflammation site and by oxidizing lipids, they produce metabolites such as 4-hydroxynonenal (4-HNE) and oxidized phospholipids (OxPLs). Transient receptor potential ankyrin 1 (TRPA1) and vanilloid 1 (TRPV1) are ligand gated ion channels that are expressed on nociceptors and their activation elicits pain. Hydrogen peroxide and 4-HNE are endogenous ligands for TRPA1 and their role in inflammatory pain conditions has been shown. OxPLs play a major pro-inflammatory role in many pathologies including atherosclerosis and multiple sclerosis. E06/T15 is a mouse IgM mAb that specifically binds oxidized phosphatidylcholine. D-4F is an apolipoprotein A-I mimetic peptide with a very high affinity for OxPLs and possess anti-inflammatory properties. E06 mAb and D-4F peptide protect against OxPLs-induced damage in atherosclerosis *in vivo.*

Methods: To investigate the role of ROS and their metabolites in inflammatory pain, I utilized a combination of diverse and complex behavioral pain measurements and binding assays. I examined E06 mAb and D-4F as local treatment options for hypersensitivity evoked by endogenous and exogenous activators of TRPA1 and TRPV1 as well as in inflammatory and OxPL-induced pain models *in vivo.* 4-HNE, hydrogen peroxide as ROS source and mustard oil (AITC) were used to activate TRPA1, while capsaicin was used to activate TRPV1.

Results: Intraplantar injection of oxidized 1-palmitoyl-2-arachidonoyl-*sn*-glycero-3-phosphocholine (OxPAPC) into rats' hind paw elicited thermal and mechanical hypersensitivity. Genetic and pharmacological evidence *in vivo* confirmed the role of TRPA1 in OxPLs-induced hypersensitivity. OxPLs formation increased in complete Freund's adjuvant (CFA)-induced inflamed rats' paw. E06 mAb and D-4F prevented OxPAPC–induced mechanical and thermal hypersensitivity (hyperalgesia) as well as CFA-induced mechanical hypersensitivity. Also, all irritants induced thermal and mechanical hypersensitivity as well as affective-emotional responses and spontaneous nocifensive behaviors. E06 mAb blocked prolonged mechanical hypersensitivity by all but hydrogen peroxide. In parallel, D-4F prevented mechanical hypersensitivity induced by all irritants as well as thermal hypersensitivity induced by capsaicin and 4-HNE. In addition, competitive binding assays showed that all TRPA1/V1 agonists induced prolonged formation of OxPLs in the paw tissue explaining the anti-nociceptive properties of E06 mAb and D-4F. Finally, the potential of gait analysis as a readout for non-provoked pain behavioral measurements were examined.

Conclusion and implications: OxPLs were characterized as novel targets in inflammatory pain. Treatment with the monoclonal antibody E06 or apolipoprotein A-I mimetic peptide D-4F are suggested as potential inflammatory pain medications. OxPLs' role in neuropathic pain is yet to be investigated.

Zusammenfassung

Im entzündeten Gewebe akkumulieren reaktive Sauerstoffspezies (ROS) sowie oxidierte Phospholipide (OxPLs). ROS und in der Reaktionskette nachgeschaltete Verbindungen, wie 4-Hydroxynonenal (4-HNE) aktivieren Transiente Rezeptor Potential (TRP) Ionenkanäle: Ankyrin 1 (TRPA1) und Vanilloid 1 (TRPV1). Diese TRP-Kanäle werden auf Nozizeptoren exprimiert und rufen Schmerz z.B. bei Entzündung hervor. OxPLs sind an vielen entzündungsfördernden Prozessen maßgebend beteiligt und spielen eine Schlüsselrolle bei Pathologie von Atherosklerose und Multipler Sklerose. E06/T15 ist ein Maus IgM-mAb, welcher spezifisch an oxidierte Phosphatidylcholine bindet. D-4F ist ein Apolipoprotein A-I (ApoA-I) mimetisches Peptid, das eine sehr hohe Affinität für OxPLs aufweist und auch entzündungshemmende Eigenschaften besitzt. E06 mAb und D-4F schützen vor Atherosklerose in vivo. Um die mögliche Rolle von OxPLs beim Entzündungsschmerz zu untersuchen, verwendete ich eine Kombination von verschiedenen und komplexen Schmerzverhaltensmessungen, Bindungsassays und immunhistologische Färbungen.

Die intraplantare Injektion von oxidiertem 1-Palmitoyl-2-arachidonoyl-sn-glycero-3-phosphocholine (OxPAPC) in die Hinterpfote der Ratte führte zu einer thermischen und mechanischen Überempfindlichkeit (Hyperalgesie). Genetische und pharmakologische Ansätze in vivo bestätigten die Rolle von TRPA1 bei OxPLs-induzierter Überempfindlichkeit. Nach Applikation von komplettem Freunds Adjuvans werden vermehrt OxPLs in der entzündeten Rattenpfote gebildet. E06 mAb und D-4F verhinderten die Ausbildung einer OxPAPC- und CFA-induzierten mechanischen und thermischen Hypersensitivität. Als nächstes untersuchte ich lokale Behandlungsmöglichkeiten der Hyperalgesie mit E06 mAb und D-4F, welche durch endogene und exogene Reizstoffe in vivo hervorgerufen wurde. Zur Aktivierung von TRPA1 wurde 4-HNE ein Lipidperoxidationsmetabolit, Wasserstoffperoxid (H_2O_2) als ROS Quelle und Senföl (AITC) genutzt. Zur Aktivierung von TRPV1 wurde Capsaicin eingesetzt. Alle diese Reizstoffe induzierten eine thermische und mechanische Hypersensitivität und spontane Schmerzreaktionen E06 mAb und D-4F inhibierten die Ausbildung einer mechanischen Überempfindlichkeit durch 4-HNE und AITC, jedoch nicht die von H_2O_2. Außerdem verhinderte D-4F die thermische Überempfindlichkeit. Alle TRPA1 und TRPV1-Agonisten führten zu der Akkumulation von OxPLs in den Hinterpfoten der Ratte.

Schlussfolgerung: OxPLs wurde als neue Zielmoleküle beim akuten und chronischen Entzündungsschmerz charakterisiert. Die Behandlung mit dem monoklonalen Antikörper E06 oder mit einem Peptid aus Apolipoprotein A-I (D-4F) verringerte die entzündungsbedingte Überempfindlichkeit und den Entzündungsschmerz.

1. Introduction

1.1 **Pain and its treatment**

Pain is described as “An unpleasant sensory and emotional experience associated with actual or potential tissue damage, or described in terms of such damage” by international association of study of pain (IASP)[1]. Although, it has evolutionarily developed to foster organism’s survival and homeostasis, pathological pain can induce excruciating suffering for the patient as well as huge economic burden for the society.

Despites decades of pain research, the transition of preclinical research data into clinical practice is occurring slowly. In recent years, only limited numbers of mechanistically novel pain medications have emerged in the market. Thus, the traditional analgesics such as opiates and nonsteroidal anti-inflammatory drugs (NSAID) stay as main agents in pain therapy for decades. However, usage of those agents is limited because of inefficiency or side effects. On the one hand, although NSAIDs are the first line medication in treatment of mild to moderate acute pain conditions, their effect is modest in treatment of severe acute and chronic pain. In addition, NSAID long-term administration is restricted because of numerous gastrointestinal and cardiovascular adverse side effects. On the other hand, despite of the potency of opioids in alleviation of severe acute pain, their utilization is limited by their life-threatening complications such as respiratory depression and apnea, unfavorable side effects such as constipation, sedation and itch as well as their potential to develop tolerance and abuse in the treated patients. Obviously, there is a critical need for novel and potent analgesics that are relying on different molecular mechanisms (Brederson, Kym & Szallasi, 2013).

1.2 **Reactive oxygen species and their downstream products**

Pain and hypersensitivity are hallmarks of inflammation that occur for instance, acutely in wounds after surgery or chronically in rheumatoid arthritis. During inflammation, macrophages and neutrophils are the main source of the reactive oxygen species (ROS) (Hackel et al., 2013; Pflucke et al., 2013). ROS consist of superoxides, peroxides and oxidative hydroxyls that possess strong oxidizing capabilities (Binder, Papac-Milicevic & Witztum, 2016; Mittal, Siddiqui, Tran, Reddy & Malik, 2014). In physiological low concentrations, ROS are constantly built and eliminated and thus contribute to cell metabolisms and signaling. However, inflammation disturbs the balance between constant production and neutralization of the intracellular ROS. This leads to ROS accumulation and oxidative stress. Oxidation of membrane lipids results in formation of neo-self-epitopes known as oxidation-specific epitopes (OSE) which are abundantly expressed by damaged or dying cells

[1] https://www.iasp-pain.org/terminology?navItemNumber=576#Pain

(Binder, 2010). Lipid peroxidation metabolites such as 4-HNE and OxPLs are critical OSE expressing bioactive molecules that represent endogenous damage-associated molecular patterns (DAMP) which are recognized by pattern recognition receptors (PRR) and proteins of the innate immune system (Tsiantoulas, Gruber & Binder, 2012). Thus, buildup of OSE can initiate an inflammatory response (Binder, Papac-Milicevic & Witztum, 2016). For instance, OxPLs bind to scavenger receptors on macrophages such as SRA1, SRA2, SRB1 and CD36 and also to toll like receptors (TLR) such as TLR-4 and stimulate the secretion of pro-inflammatory IL-6 by the macrophages.

OxPLs can be produced via two different mechanisms, either direct oxidation or reesterification pathway. Phospholipids can be oxidized enzymatically by 12/15-lipoxygenases or be oxidized by ROS or reactive nitrogen species (RNS). OxPLs with full-length or shortened carbon chains can be produced from the primary oxidation products (hydroperoxides) via rearrangements, oxidation, cyclization or fragmentation. Numerous OxPL species are synthesized from non-enzymatic oxidation of one individual precursor PL. The second possible pathway is reesterification pathway in that, free fatty acid (e.g., arachidonic acid) is oxidized by lipoxygenases or cyclooxygenases with formation of free eicosanoids, which can be further reesterified into PLs (**Figure 1**).

In conclusion, complexity of lipid mixtures is dramatically increased by oxidation of PLs and production of a variety of oxidized molecular species. Pleiotropic biological activities of OxPLs could be explained by this diversity of chemical structures and reactivities of OxPLs (Bochkov, Gesslbauer, Mauerhofer, Philippova, Erne & Oskolkova, 2017).

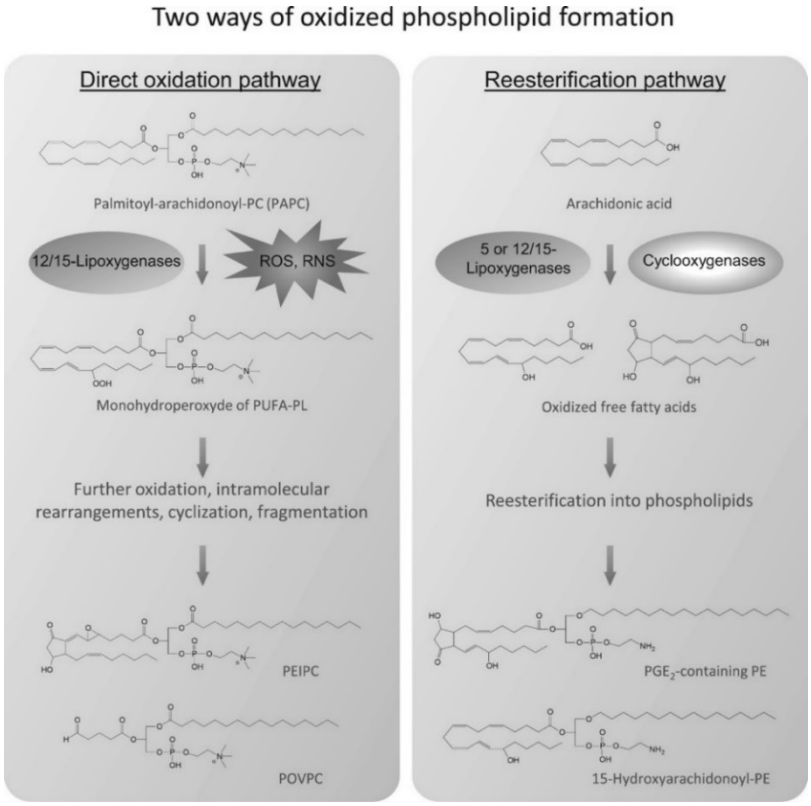

Figure 1 Pathways of OxPL production. Adapted from (Bochkov, Gesslbauer, Mauerhofer, Philippova, Erne & Oskolkova, 2017)

1.3 **OxPLs in pathophysiology**

OxPLs are highly reactive chemicals and trigger diverse pro- and anti-inflammatory pathways. In atherosclerosis, OxPLs play a major pro-inflammatory role. For instance, they promote adhesion of monocytes to endothelial cells and transformation of macrophages into foam cells which contains oxidized low-density lipoprotein (OxLDL). Also, they support plaque formation and chemokine production (Dickhout, Basseri & Austin, 2008; Lee, Birukov, Romanoski, Springstead, Lusis & Berliner, 2012). In contrast, OxPLs block lipopolysaccharide (LPS)-induced activation of TLR-2 and TLR-4 (Bochkov, Oskolkova, Birukov, Levonen, Binder & Stöckl, 2009; Erridge, Kennedy, Spickett & Webb, 2008) or simply activate TLR-2 possibly in complexes with CD36 (Seimon & Tabas, 2009; Seimon et al., 2010). Not only OxPLs are well known mediators in pathophysiology of atherosclerosis, but also are known to play a role in acute inflammation for instance in acute lung injury or sepsis (Imai et al., 2008) and chronic inflammatory or neurodegenerative diseases such as Alzheimer's and Parkinson's (Leitinger, 2008; Qin, Goswami, Balabanov & Dawson, 2007; Usui, Hulleman, Paulsson, Siegel, Powers & Kelly, 2009).

One of the commercially available and routinely studied mixture of OxPLs is oxidized 1-palmitoyl-2-arachidonoyl-*sn*-glycero-3-phosphocholine (OxPAPC) which consists of a mixture of oxidized, chain-shortened phospholipids including 1-palmitoyl-2-(5-oxovaleroyl)-*sn*-glycero-3-phosphocholine (POVPC) and 1-palmitoyl-2-glutaryl-*sn*-glycero-3-phosphocholine (PGPC) as well as oxygenated phospholipids such as 1-palmitoyl-2-(5,6)-epoxyisoprostaneE_2-*sn*-glycero-3-phosphocholine (PEIPC) (Bretscher et al., 2015). OxPAPC species have been previously detected in inflammation, but its role in inflammatory pain was entirely unknown until recently (Bochkov, Oskolkova, Birukov, Levonen, Binder & Stöckl, 2009; Liu et al., 2016). Although the majority of OxPLs species are pro-inflammatory, it should be noted that some epoxycyclopentenone components of OxPAPC possess anti-inflammatory bioactivity (Bretscher et al., 2015). So, there is a cross-talk between upregulation of ROS and their down-stream molecules on the one hand and inflammatory response on the other hand.

1.4 **E06/T15 mAb**

E06 mAb specifically binds to phosphocholine (PC) head group of oxidized phospholipids (Friedman, Hörkkö, Steinberg, Witztum & Dennis, 2002). It is identical to T15, a natural IgA form B-1 cell origin that protects against *S. pneumoniae* infections (Masmoudi, Mota-Santos, Huetz, Coutinho & Cazenave, 1990; Shaw et al., 2000). E06 possess some strong anti-inflammatory and pro-resolving properties. Passive and active immunization by E06 protects against atherosclerotic plaque development (Binder et al., 2003; Faria-Neto et al., 2006) by facilitating apoptotic cells clearance (Shaw et al., 2000). Furthermore, E06 neutralizes pro-inflammatory effects of OxPLs on macrophages by blocking their attachment to scavenger receptors and TLRs (Imai et al., 2008).

Considering the critical role of OSEs in development of inflammatory conditions, understanding the underlying molecular mechanisms of OSE-induced inflammation as well as determining the potency of natural anti-OSE compounds such as E06/T15 type mAb in antagonizing inflammatory conditions will contribute to the development of novel therapeutic interventions.

It should be noted that E06 mAb is not the only Ab specific for OxPLs. DLH3 and 509 are also mAb specific for OxPLs. DLH3 was isolated from BALB/c mice that were immunized with homogenates of human atheromatous plaques of aortae (Itabe et al., 1994) and the mAb 509 was generated by immunizing mice with a mixture of OxLDL and OxPAPC (Bochkov et al., 2016). While DLH3 mAb similar to E06 mAb binds to oxidized phosphatidylcholine, 509 mAb recognizes oxidized phosphatidylethanolamine (Bochkov et al., 2017).

Recently it was shown that expression of a single-chain variable fragment of E06 (E06-scFv) using the Apo-E promoter to inactivate OxPLs is beneficial for reducing generalized inflammation, including the progression of atherosclerosis, aortic stenosis and hepatic steatosis (Bochkov et al., 2017). E06-scFv also protects against high-fat diet-induced bone loss by increasing osteoblast number and stimulating bone formation and increases bone mass in mice fed a normal diet (Bochkov et al., 2017).

1.5 D-4F an Apo-A mimetic peptide

A mimetic peptide is defined as a rather small peptide (14-20 amino acids) that biologically mimics the properties of bioactive macromolecules such as hormones, cytokines, enzyme substrates, viruses or other biomolecules. Apolipoprotein A-I (ApoA-I), a structural protein of the high density lipoproteins and its mimetic peptide D-4F reduce atherosclerotic plaque formation ,OxPLs quantities and pro-inflammatory reactions of low density lipoproteins (LDL) (Getz, Wool & Reardon, 2010). 4F peptides that are a group ApoA-I mimetic peptides are synthesized from both all D-amino acids (D-4F) and all L-amino acids (L-4F). D-4F (Ac-DW F KA F YDKVAEK F KEA F NH 2) is an amphipathic and helical peptide that functions as an apoA-I mimetic. Also, there are accumulating evidences showing its favorable effect on other autoimmune diseases such as scleroderma, collagen-induced arthritis or systemic lupus (Frostegard et al., 2005) (Charles-Schoeman et al., 2008). While concentration of apoA-I (a 28-kDa protein) in human and mouse plasma is approximately 35 μM, D-4F has a molecular weight of 2.3 kDa and its maximal plasma concentration achieved by oral administration to mice is approximately 130 nM. D-4F has a much higher affinity for OxPLs in comparison to ApoA-I (Van Lenten et al., 2008) and protects against oxidative stress and inflammation in a murine asthma model (Nandedkar et al., 2011). Interestingly, D-4F treatment decreases E06/T15 immunoreactivity and accumulation of 4-HNE and 4-HNE protein adducts which both are metabolites of lipid oxidation (Buga et al., 2008; Nandedkar et al., 2011).

1.6 **Na_v 1.9 voltage-gated sodium channels**

$Na_V1.9$ is a voltage-gated sodium channel (VGSC) that is particularly expressed in peripheral nervous system and is believed to play a role in pain transduction (Leo, D'Hooge & Meert, 2010). $Na_V1.9$ regulates the excitability of the neuron and it is suggested that the increased excitability of the nociceptors during inflammation may be orchestrated by $Na_V1.9$ (Östman, Nassar, Wood & Baker, 2008).

1.7 **ROS and their downstream products as activators of TRPA1**

ROS and their downstream products themselves are pro-nociceptive through activation of transient receptor potential vanilloid 1 (TRPV1) or ankyrin 1 (TRPA1) receptors in sensory neurons. Accumulation of ROS and their metabolites is a crucial part of any inflammatory response (Binder, Papac-Milicevic & Witztum, 2016). In addition, ROS promote inflammatory and neuropathic hypersensitivity and spontaneous nociception partly by activating TRPA1 and TRPV1 channels (Andersson, Gentry, Moss & Bevan, 2008; Keeble et al., 2009; Trevisan et al., 2016). ROS-mediated TRPA1 and TRPV1 activation is the suggested underlying mechanism of many painful pathologies such as gouty arthritis (Trevisan, Hoffmeister, Rossato, Oliveira, Silva & Ineu, 2013), trigeminal neuropathic pain (Trevisan et al., 2016) and photosensitization in porphyrias and photodynamic therapy side effects (Babes, Sauer, Moparthi & Kichko, 2016). TRPA1 and TRPV1 are polymodal transmembrane nonspecific cation channels, critically involved in nociception (Kaneko & Szallasi, 2014; Stucky, Dubin, Jeske, Malin, McKemy & Story, 2009). TRPA1 is widely co-expressed with TRPV1 on a subset of Aδ and C fibers of nociceptors which upon activation readily release pro-inflammatory agents such as CGRP and substance P (SP) among others and induces neurogenic inflammation (Koivisto et al., 2014; Viana, 2016). TRPA1 and TRPV1 are also functionally expressed on non-neuronal cells such as synoviocytes (Kochukov, McNearney, Fu & Westlund, 2006), and chondrocytes (Nummenmaa et al., 2016; Somogyi et al., 2015). An important role of TRPA1/V1 channels in pathology of arthritis has been suggested (Pereira et al., 2017; Trevisan et al., 2013a). TRPA1 is activated by wide range of electrophile and non-electrophile endogenous and exogenous compounds as well as noxious cold (Viana, 2016). Electrophiles, such as allyl isothiocyanate (AITC, also known as mustard oil), H_2O_2 and downstream products of lipid peroxidation such as 4-hydroxynonenal (4-HNE) activate TRPA1 via covalent modification of cysteine residues of N-terminus of the protein (Liu et al., 2016; Paulsen, Armache, Gao, Cheng & Julius, 2015; Trevisani et al., 2007b). Also, TRPA1-mediated cold hypersensitivity and post-incisional guarding is transduced via ROS signaling (Miyake et al., 2016; Sugiyama, Kang & Brennan, 2017). TRPV1 is activated by capsaicin, extreme pH, noxious heat (Ogawa et al., 2016; Stucky, Dubin, Jeske, Malin, McKemy & Story, 2009). In **figure 2**, a scheme of peripheral sensitization at nociceptors and the main role players in development of such sensitization is shown (Gangadharan & Kuner, 2013).

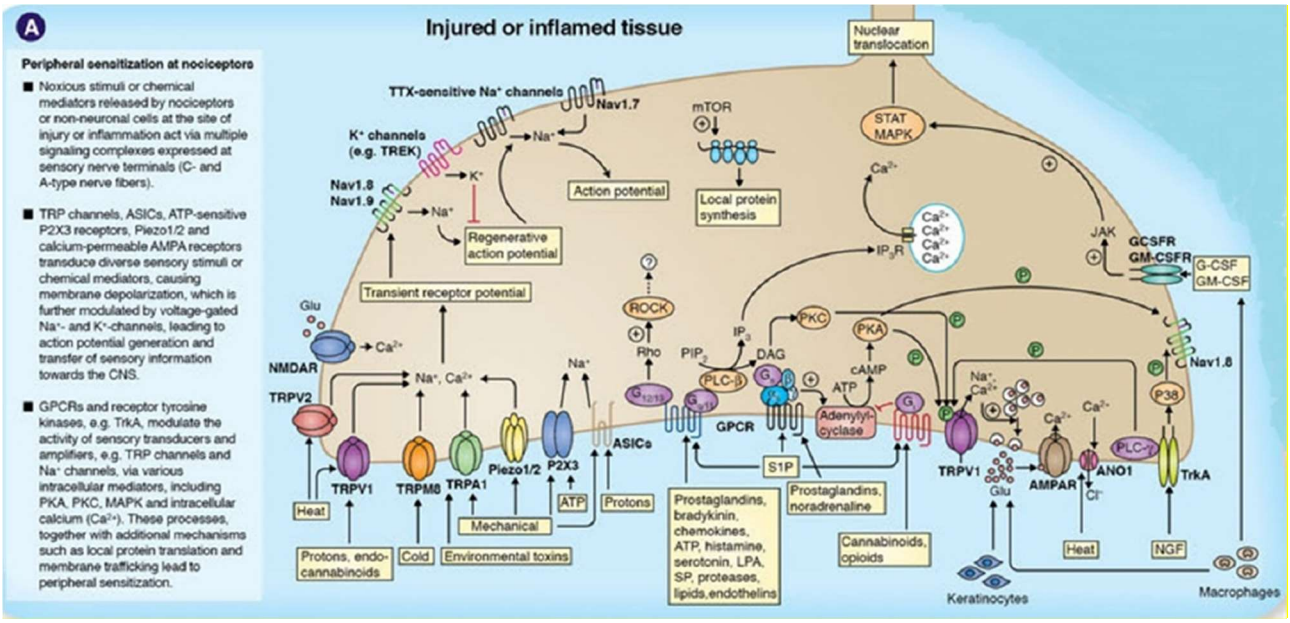

Figure 2 Peripheral sensitization at nociceptors
adopted from (Gangadharan et al., 2013)

1.8 **Aim of the present study**

Recently, it was shown that OxPLs activate heterologous and native TRPA1 *in vitro*. Also, it is known that E06/T15 mAb and D-4F peptide protect against pro-inflammatory activity of OxPLs (Faria-Neto et al., 2006; Hörkkö et al., 1999). OxPLs-mediated activation of TRPA1 could be blocked by co-application of E06 *in vitro (Oehler et al., 2017a)*. Considering this, in current study, I aimed to determine the role of OxPLs in inflammatory pain and potential of E06 mAb and D-4F peptide in blocking such pain as well as determining the specificity of antinociceptive properties of E06 mAb and D-4F peptide downstream of TRPA1 and TRPV1 activation.

2. Materials and Methods

2.1 **Materials**

2.1.1 Animals

All animals were accommodated in groups of three to six under standard conditions (12 h: 12 h light/dark cycle, 21-25°C, 45-55% humidity) with food and water *ad libitum*. Upon arrival, they were acclimated to the new environment for at least 7 days before handling started. All handling procedures were in accordance with international guidelines for the care and use of laboratory animals (EU Directive 2010/63/EU for animal experiments). All animal experiments were approved by the government of lower Franconia protocol number 61/11(Mohammadi et al., 2014; Mohammadi & Fendt, 2015).

Male Wistar rats (200-300 g) were purchased from Janvier Labs, Le Genest-Saint-Isle, France. Na_v 1.9 KO and C57BL/6J wild type (WT) mice were bred in Institute of Clinical Neurobiology, University of Wuerzburg, Germany (Östman, Nassar, Wood & Baker, 2008). Initial TRPA1 KO mice were a generous gift from Drs Kwan and Corey (Kwan et al., 2006).

TRPV1 KO mice were donated by Dr. Davis (Davis et al., 2000). TRPA1 KO and TRPV1 KO mutant mice were bred in the Institute of Physiology and Pathophysiology, University of Erlangen, Germany. By end of the experiments, the animals were euthanized by asphyxiation in CO2 or cervical dislocation. Animals were randomly assigned to treatment groups and the experimenter was blinded to the treatments and genotypes (Oehler et al., 2017a; Oehler et al., 2017b).

2.1.2 Chemicals, compounds, consumables and buffers

Name	Company	Catalogue number
4-HNE	Alpha Diagnostic International	HNE51-1
4-HNE-BSA	Cell Biolabs	STA-335
AITC	Sigma	W203408
Aqua PolyMount	Polysciences	18606-100
BCTC	Sigma	SML0355
Black flat bottom Microfluor 1 96 wells plates	Thermo scientific	7605
Black OxPC snoopers ®	Avanti	330602
Bovine serum albumin	Sigma	05470
Capsaicin	Sigma	M2028
CFA	Calbiochem	344289
Chloroform	Sigma	C2432

D-4F peptide	Peptide 8 Specialty Labs	custom-made
DAPI	Sigma	D9542
DMSO	Sigma	W387520
Dulbecco`s PBS	PAA Laboratories	SH30028.01
E06 mAb	Avanti	330003
EDTA	Merck	324506
Ethanol	Sigma	46139
Goat serum	Sigma	G9023-5ML
H_2O_2	Sigma	H1009
HC-030031	Sigma	H4415
Isoflurane	CP pharma	CDS019936
Methanol	Sigma	322415
Mouse IgM isotype control	Biomol	ADI-SAB-600-485
OxPAPC	Hycultech	HC4036
Paraformaldehyde	Sigma	158127
PC-BSA	Biosearch Technologies	PC-1011-10
Sucrose	Sigma	S9378
SuperFrost™	Thermo scientific	9951TPLUS
TissueTek	Sakura Finetek	25608-930
Triton-X 100	Sigma	X100
Tween 20	Sigma	P1379

Table 1 Chemicals, compounds, consumables and buffers together with their catalogue numbers and producers

2.1.3 Equipment

von Frey filaments	North Coast Medical Inc., Gilroy, USA
Paw pressure algesiometer (modified Randall-Selitto test)	Ugo Basile, Comerio, Italy
Plantar test apparatus	IITC Life Science Inc., Woodland Hills, USA
CatWalk XT	Noldus Information Technology Inc., Wageningen, Netherlands
Plethysmometer	Ugo Basile, Comerio, Italy
Sonifier	IKA® RW 14, IKW®-Werke, Staufen, Germany
Genios pro Fluorecence plate reader	Tecan group ltd., Maennedorf, Switzerland
Cryostat	Leica, Wetzlar, Germany

Table 2 Main equipment and their producers

2.1.4 Buffers for binding assay

Direct assay washing buffer	0.1% Tween 20 In 1X PBS
Competitive assay washing buffer	1X PBS
Blocking solution	2% BSA 0.27 mM EDTA In 1X PBS

Table 3 Formulations of the buffers which were used in binding assays

2.1.5 Buffers for immunohistochemistry

Fixative solution	(4% PFA, 30% sucrose) 4 g paraformaldehyde 30 g sucrose 1 L PBS dissolve at 60°C
Embedding	Tissue-Tek
Blocking solution	5% goat serum or 2% BSA 0.1% Triton-X 100 0.1% Tween 20
Washing solution	0.1% Tween 20 In 1X PBS
Mounting medium	Aqua PolyMount

Table 4 Buffers and media which were used in immunohistochemistry

2.1.6 Primary antibodies used for immunofluorescence

Clone	labeling	Type	Host	Against	Working dilution	Company	Cat. No.	Stock dilution
RP-1	granulocytes	mAb IgG2	Mouse	Rat	(1/600)	BD Pharmingen	550002	0.2 mg/ml
ED-1	macrophage /monocytes	mAb IgG1	Mouse	Rat	(1/600)	ABD Serotec	MCA341R	0.25 mg/ml
E06	OxPLs	mAb IgM	Mouse	Rat	(1/100) - (1/1200)	Avanti Polar Lipids	330001	1 mg/ml
TEPC 183 (isotype)	unknown	mAb IgM ƙ	Mouse	unknown	(1/100) - (1/1200)	Ancell	290-810	1 mg/ml

Table 5 List of primary antibodies which were used for immunofluorescence

2.1.7 Secondary antibodies used for immunofluorescence

Antibody	Host	Stock Dilution	Working dilution	Company	Cat. No.
Alexa Fluor® 488 anti-Mouse IgG (H+L) F(ab) Fragment	goat	1:1 in glycerol 0.5 mg/ml	1:600	Jackson	115-547-003
Cy3® anti-mouse IgM heavy chain specific	goat	1.5 mg/ml	1:600	Jackson	115-165-020
Cy3® Anti-Mouse IgG (H+L) F(ab) Fragment	goat	1:1 in glycerol 0.5 mg/ml	1:600	Jackson	115-167-003

Table 6 List of secondary antibodies which were used for immunofluorescence

2.1.8 Software

Microsoft Office 2010, Excel, Word, Power Point	CatWalk XT10.50
Adobe Photoshop 7.00	Endnote X7
Movie Studio Platinum 13.00	ImageJ, Fiji
Xilisoft AVCHD Converter	SigmaPlot 13.00

Table 7 Software which were used for data analysis and presentation

2.2 Methods

2.2.1 Behavioral testing

2.2.1.1 Taxonomy

In order not to overgeneralize animal behaviors in addressing pain-like and relief-like behaviors, I used a taxonomy that is suggested by International Association for the Study of Pain (IASP) (Corder et al., 2017; Mogil, 2009). Rodent's pain-like behaviors can be categorized to nociceptive withdrawal reflexes, affective-emotional responses and spontaneous nocifensive behaviors. Nociceptive withdrawals are fast reflexive retractions of the hind paw in response to nociceptive sensory input which can be provoked by either mechanical or thermal stimuli. Once the threshold of nociceptive reflexes to mechanical or thermal stimuli is reduced, that could be considered as mechanical or thermal hypersensitivity, respectively. Affective-emotional responses are temporally delayed intentional licking and guarding of the affected hind paw. On the contrary, spontaneous nocifensive behaviors are non-evoked flinches of the affected hind paw that can be attributed to spontaneous nociception. These behaviors are relying on different neural mechanisms and pathways. While nociceptive reflexes are mediated via spinal centers and without modulation by the brain, affective-emotional responses are mainly transduced via cortex and upper nervous system. Thus, I avoided frequently used taxonomy such as "allodynia" and "hyperalgesia" when referring to animal's behavior and substitute them with "hypersensitivity" in such context (Mohammadi *et al.*, 2018).

2.2.1.2 Measurement of mechanical hypersensitivity to light touch

Von Frey (VF) filaments are a type of aesthesiometer that were first introduced in 1896 by Maximilian von Frey. They are ever since used in clinical and research purposes to measure mechanical touch hypersensitivity. Here, hypersensitivity was investigated using the up-down method for calculating the 50% threshold using VF hairs as previously described (Chaplan, Bach, Pogrel, Chung & Yaksh, 1994). Briefly, mice were individually put in transparent Plexiglas chambers over a wire mess platform and acclimated to the test room for at least 60 min. Then, the VF filaments were applied to the plantar surface of the hind paw through the mesh from below, starting at filament number five. Vigorous paw withdrawal was considered as reflexive nociceptive behavior and a positive trial. Each filament was applied at least three times and at least 30 s apart. Once two out of

three trials were positive the response was considered positive and the next filament with the higher number was applied. In case of a negative response, the next filament with the lower number was used. In case of an inconclusive response, the trial was repeated. The sequence was continued for four more responses after the first positive response. Then the resulting pattern of the responses was used to calculate the 50% threshold using the following formula:

$$50\%\ \text{g threshold} = \frac{10^{(Xf+\kappa\delta)}}{10{,}000}$$

Where Xf = value of the last applied filament; κ = tabular value of the pattern of the responses (appendix 1) and δ = mean difference between the filaments.

The calculated 50% threshold for each animal was used to make a mean threshold for the animals with the same treatment and in same time point. Then the means were analyzed using repeated measures analysis of variance (RM ANOVA), followed by Holm-Sidak (H-S) multiple comparison post-hoc analysis to find the significant differences across treatments and time point as well as their interaction (Oehler et al., 2017a).

2.2.1.3 Measurement of mechanical pressure hypersensitivity

The paw pressure algesiometer was used for measuring paw pressure threshold (PPT) (Randall & Selitto, 1957). Reduction of PPT was considered as indicator of mechanical pressure hypersensitivity. The test is based on determination of the animal's reflexive nociceptive thresholds to application of a gradually increasing pressure via a conic blunt tip (1 mm diameter) on the rats' hind paw. Male Wister rats were handled one by one for three to five days before start of the measurements. At time of the experiment, they weighted 200-300 g. For each animal, PPT was measured at 0 (baseline), 1, 3 and 6 h after intraplantar injection of the reagents in the rats' hind paw. At each time point PPT was measured three to five times for each animal and a mean was calculated for the time point and individual animal. Finally, a mean and standard error of the mean (SEM) of the PPT of different animals in the same time point was calculated and analyzed with RM ANOVA, followed by Holm-Sidak post-hoc analysis and statistically significant differences between groups and time points were recorded (Hackel et al., 2012; Oehler et al., 2017a; Rittner et al., 2009).

2.2.1.4 Measurement of thermal hypersensitivity

Thermal reflexive nociceptive thresholds were measured as paw withdrawal latency (PWL) using the plantar test apparatus (Hargreaves, Dubner, Brown, Flores & Joris, 1988). Animals were individually accommodated in Plexiglas transparent enclosures with a glass floor and were allowed to habituate for 30 min. then a beam of radiated heat was focused on the hind paws and the latency to withdrawal was recorded. The intensity of the beam was adjusted to gain a mean of 12 s PWL for a non-treated paw and a cut-off latency time of 20 s was used to avoid tissue damage. Each

measurement was apart by at least 30 sec, three measurements were performed for each time point and hind paw. The measurements were repeated on 0 (baseline), 1, 3 and 6 h after injections. The mean PWLs were calculated for each time point and treatment (Oehler et al., 2017a; Pflucke et al., 2013; Rittner et al., 2009).

2.2.1.5 Measurement of spontaneous nociception

Animals were restrained gently and the mixture of the intended reagents was intraplantarly injected. Afterwards, the animal was placed in a transparent Plexiglas chamber on glass floor and watched by an experimenter blinded to the treatment for 10 min and the duration of spontaneous nocifensive flinching and affective-motivational behaviors such as guarding and licking of the treated paw were recorded with a stopwatch (Tappe-Theodor & Kuner, 2014).

2.2.2 Gait analysis

There is currently a lack of predictive power for drug effect using conventional mechanical and thermal nociceptive threshold measurements. Furthermore, gait analysis provides a more objective way to measure pain and might be more clinically relevant. Therefore, functional methods are gaining popularity or are increasingly necessary (Tappe-Theodor & Kuner, 2014).

Gait characteristics were recorded by CatWalk XT. Male Wistar rats (200-250 g) were trained and handled for 10 days before baseline recordings. As shown in the experiment outline (**Figure 3**), the animal was injected with 150 µl CFA in the ipsilateral hind paw after the baseline recording. Each trial consisted of between 1-5 runs depending on quality of the particular animal behavior. All animals were recorded again 3 and 24 h after CFA injection. Then 3 µg fentanyl in 100 µl saline was injected into the ipsilateral hind paw of the experimental group and the control group received vehicle. After 15 min, the animal's gaits were recorded. Forty-eight hours after CFA treatment runs were recorded and then 500 µg D-4F peptide in 100 µl saline was injected into the ipsilateral hind paw of the experimental group and the control group received vehicle. After 3 h, gait behavior was recorded for the last time then animals were euthanized.

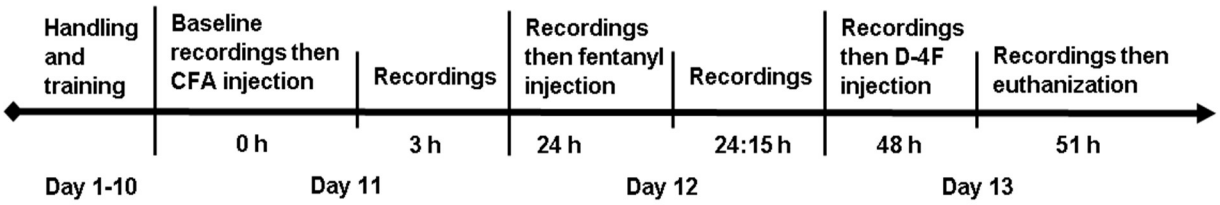

Figure 3 Outline of the experimental procedure for gait analysis

2.2.3 Measurement of paw volume and edema

Baseline measurements were recorded before injections and at the indicated time points thereafter for ipsilateral and contralateral paws. Paw edema was determined by placing hind paws in a water-filled Perspex cell of a plethysmometer. Averages from three measurements per treatment and time point were calculated (Oehler et al., 2017a).

2.2.4 Lipid extraction

Rat plantar hind paw soft tissue was dissected leaving tendons and bones in place, skinned and snap-frozen in liquid nitrogen, and kept in -80°C till extraction. The extraction was performed by a modified Folch extraction procedure (Folch, Lees & Stanley, 1957; Watson et al., 1997). Whole paw tissue was weighted, minced and homogenized in chloroform, methanol and water cocktail (volume 2:1:1) using a sonifier. After centrifugation at 1500 g, 4°C, 30 min, the chloroform phase containing lipids was retrieved and evaporated under nitrogen. Extracted lipids were immediately used in binding assays (Oehler et al., 2017a).

2.2.5 Binding assays

For determining *ex vivo* quantities of OxPLs in extracted lipids from rat paws as well as for evaluation of E06 mAb binding with different synthetic compounds, direct and competitive binding assays were performed. For blocking non-specific bindings, 2% BSA, 0.27 mM EDTA in PBS (250 µl) was used. Unless otherwise mentioned, PBS (250 µl) was the washing solution. Samples were run in duplicates and the mean fluorescence intensity (FI) for each sample was quantified and calculated with excitation at 485 nm and read out at 520 nm using a Tecan Genios pro Fluorecence plate reader. For the analysis of unknown samples, the standard curve was calculated and drawn with a titer of synthetic OxPAPC (0.032-20 µg,) using a four-parameter logistic curve regression model (Chattopadhyay et al., 2016; Watson et al., 1997). For probing the binding potency of E06 mAb to the synthetic chemicals (OxPAPC, 4-HNE and 4-HNE-BSA), relative FI changes was calculated as percentage of negative samples (only PBS) FI for each sample using formula:

$$\text{FI relative change} = \frac{\text{chemical's mean FI}}{\text{negetive sample's mean FI}} \text{x}100 - 100.$$

2.2.5.1 Competitive binding assay

Black OxPC snoopers ® (ELISA well strips, pre-coated with OxPC species) were blocked with the blocking solution for 45 min on RT and then washed 3X. Lipid samples were emulsified in 50 µl PBS and mixed with 50 µl of E06 mAb TopFluor (2 $\mu g.ml^{-1}$ in blocking solution) and incubated on OxPC strips for 1 h RT. After washing 4X, fluorescence intensity was quantified (Oehler et al., 2017a).

2.2.5.2 Direct binding assay

Black flat bottom Microfluor 1 96-wells plates were coated with emulsified samples in 100 µl PBS overnight (ON) at 4°C. Then, the wells were washed twice and blocked for 1 h on RT. After two further washings, 100 µl of E06 mAb TopFluor (1.25 $\mu g.ml^{-1}$ in blocking solution) was added to each well and incubated for 1 h RT. Finally, after washing 4X in 0.1% TWEEN 20 in PBS, fluorescence intensity was quantified (Oehler et al., 2017a).

2.2.6 Immunohistochemistry

Rat hind paw soft tissue was dissected and fixed overnight (ON) in the fixative solution. Then the tissue was washed 3X in PBS and was imbedded in Tissue-Tek medium.

Using a cryostat and on -19 to -22 °C serial section with 10-25 µm thickness were made and immobilized on SuperFrost™ slides. The slides were washed in 1X PBS for 10 min and then were permeabilized and blocked with the blocking solution for 2 h. After tapping the excess blocking solution, primary antibody was incubated on the slides ON 4°C. The day after, the slides were washed 3X in washing solution and the secondary antibody was applied for 1.5 h on room temperature (RT). Afterwards, the excess antibody was removed and DAPI was incubated on the slides for 10 min in RT. ultimately, the slides were washed 3X in the washing solution and the slides were embedded in the mounting medium and were cover slipped.

2.2.7 Statistical analysis

Results were reported as mean scores ± standard error of the mean (SEM). SigmaPlot 13 (Systat Software Inc.) was used for the analysis of the *in vivo* data and the binding assay. All data sets were tested for normal distribution (Shapiro-Wilk test) and equality of variance (Brown-Forsythe test). I used two-way repeated measurement ANOVA followed by Holm-Sidak post-hoc multiple comparison test for behavioral prolonged hypersensitivity data and one-way ANOVA with Holm-Sidak post-hoc multiple comparison test for acute nociception and OxPLs quantification data.

3. Results

3.1 Synthetic OxPAPC as a proalgesic agent and its antagonization by E06 mAb

3.1.1 E06 mAb dose dependently blocks OxPAPC-induced mechanical hypersensitivity

It was already shown that OxPAPC, dose dependently induces mechanical hypersensitivity (Oehler et al., 2017a). I tested whether co-incubation of E06 mAb that is known to specifically binds to OxPLs can prevent OxPAPC-induced mechanical hypersensitivity. Different doses of E06 mAb (0.2-1 µg) or IgM isotype control (1 µg) or saline was pre-incubated with 500 µg OxPAPC for 10 min. Then under a brief anesthesia by isoflurane, the mixture was intraplantarly injected into the rats' hind paw. PPT was measured at 0 (baseline), 1, 3 and 6 h post-injection. OxPAPC decreased PPT and induced mechanical hypersensitivity in a time-dependent manner. In saline, IgM isotype and E06 mAb 0.2 µg groups, PPT reached its minimum 3 h after the injection and increased again 6 h after the injection. On contrary, PPT in E06 mAb 1 µg group just slightly decreased and PPT in E06 mAb 0.5 µg group did not decrease as strong as the control groups. In comparison to IgM isotype and saline groups, PPT was significantly higher in E06 mAb 1 µg and 0.5 µg groups 3 h after injection. Mechanical thresholds on the contralateral paws were not significantly altered throughout the experiment (**Figure 4**) (Oehler et al., 2017a).

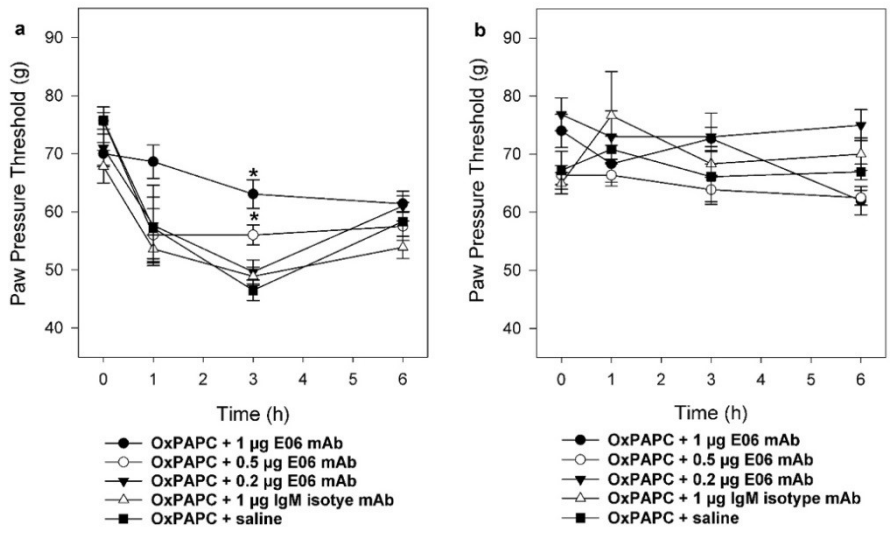

Figure 4 Dose-dependent inhibition of OxPAPC-induced mechanical hypersensitivity by E06 mAb

E06 mAb but not IgM isotype control dose-dependently prevents OxPAPC-induced mechanical hypersensitivity (a) without affecting contralateral paw (b). Different doses of E06 mAb and the highest dose of IgM isotype control and saline were incubated with 500 µg OxPAPC and were injected intraplantarly after baseline measurement. Paw pressure thresholds were recorded before injection (baseline) and 1, 3 and 6 h after injections. Data is shown as mean paw pressure threshold for each treatment group +/- SEM. N = 5-6/group, Two-way RM ANOVA, * $p < 0.05$. Versus IgM isotype control within the time point.

3.1.2 Calculation of the optimal dose of E06 mAb

To find the optimum dose of E06 mAb for behavioral experiments, I performed a four-parameter logistic regression analysis. Based on dose-dependent responses of E06 mAb on OxPAPC-induced mechanical hypersensitivity at 3 h time point, it was revealed that 1.2 µg of E06 mAb will theoretically block hypersensitivity induced by 500 µg (**Figure 5**). Considering R^2 = 0.9315 and confidence interval of 4, Assumed a dose of 1.2 µg of E06 mAb would be the premium dose to abolish the biological effects of OxPLs *in vivo*.

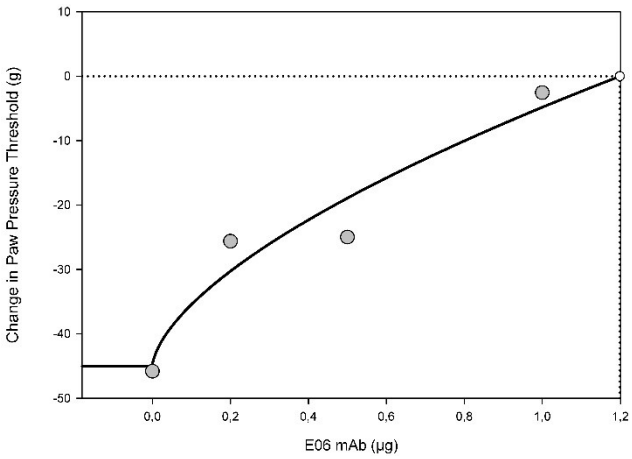

Figure 5 Theoretical modeling of anti-nociceptive effects of E06 mAb using a four-parameter logistic regression model

Anti-nociceptive effects of E06 mAb using a four-parameter logistic regression model is estimated, N = 6.

3.1.3 E06 mAb alone has no effect on thermal and mechanical thresholds

To explore the possible algetic or anesthetic effects of E06 mAb on non-inflamed rats' paw, I injected 1 µg of E06 mAb and measured PPT and PWL at 0 (baseline), 1, 3 and 6 h after injection. As shown in (**Figure 6**), PPT and PWL values did not significantly change over 6 h (Oehler et al., 2017a).

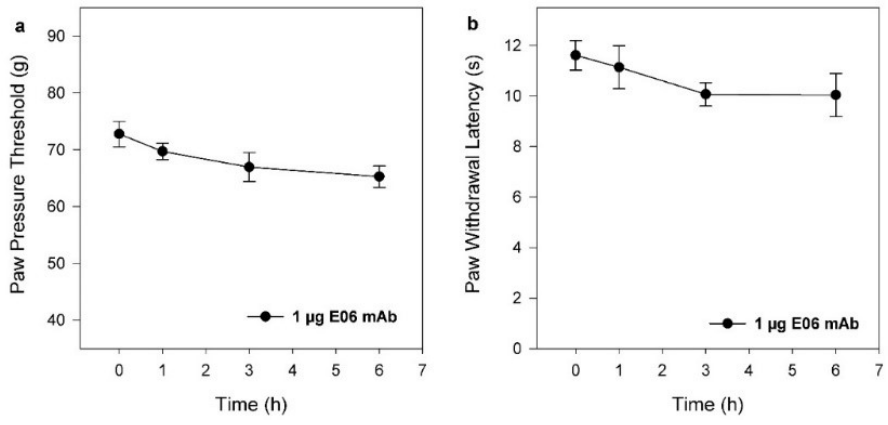

Figure 6 No effect of intraplantar E06 mAb on thermal or mechanical thresholds

Intraplantar injection of 1 µg E06 mAb into rats' hind paw does not alter mechanical (**a**) or thermal (**b**) nociceptive thresholds over 6 h. Paw pressure thresholds and paw withdrawal latencies were recorded before injection (baseline) and 1 h, 3 h and 6 h after injections. Data is shown as mean paw withdrawal latency and mean paw pressure threshold for each treatment group +/- SEM. N = 6/group, Two-way RM ANOVA, $p > 0.05$.

3.1.4 OxPAPC-induced thermal hypersensitivity is prevented by E06 mAb

After showing that coincubation of E06 mAb can prevent development of mechanical hypersensitivity induced by OxPAPC, I asked this question whether OxPAPC-induced thermal hypersensitivity could be blocked by pre-coincubation of E06 mAb. E06 mAb (1 µg) or IgM isotype control (1 µg) or saline were pre-incubated with 500 µg OxPAPC for 10 min. Then the mixture was intraplantarly injected into the rats' hind paw under a brief anesthesia by isoflurane. PWL was measured at 0 (baseline), 1, 3 and 6 h post-injection. In IgM isotype and saline groups, OxPAPC decreased PWL and induced thermal hypersensitivity. Coincubation of E06 mAb with OxPAPC blocked the development of thermal hypersensitivity with a significant difference in regard to IgM isotype and saline groups 3 h after the injection. Thermal nociceptive thresholds returned to normal range 6 h after the injection in all groups (**Figure 7**) (Oehler et al., 2017a).

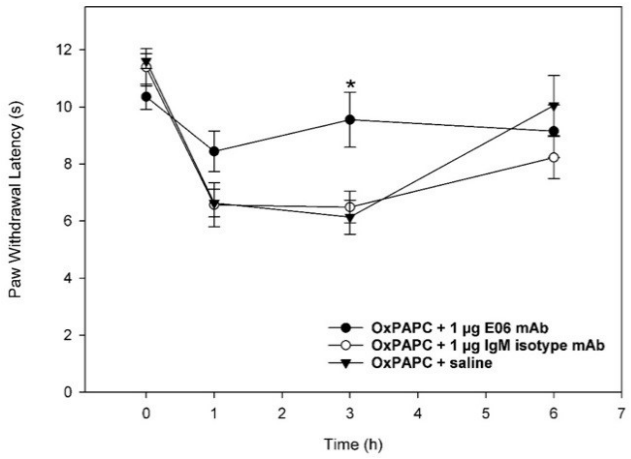

Figure 7 Blockage of OxPAPC-induced thermal hypersensitivity by E06 mAb

Intraplantar injection of 500 µg OxPAPC co-incubated with either 1 µg IgM isotype or saline but not 1 µg E06 mAb into rats' hind paw leads to thermal hypersensitivity. Paw withdrawal latencies were recorded before injection (baseline) and 1, 3 and 6 h after injections. Data is shown as mean paw withdrawal latency for each treatment group +/- SEM. N = 6/group, Two-way RM ANOVA, post-hoc Holm-Sidak, *p < 0.05 versus IgM isotype or saline within time point.

3.1.5 OxPAPC-induced mechanical hypersensitivity in TRPA1 KO but not TRPV1 KO mice and no thermal hypersensitivity

To specifically evaluate the role of TRPA1 and TRPV1 ion channels in OxPAPC-induced mechanical hypersensitivity, TRPA1 KO, TRPV1 KO and WT littermates were intraplantarly injected with 100 µg OxPAPC in 50 µl saline. Mechanical thresholds were measured using von Frey filaments before injections (baseline) as well as 1, 3 and 6 h after the injection. OxPAPC elicited mechanical hypersensitivity in all animals after injection. OxPAPC injection lead to significantly reduced mechanical hypersensitivity in TRPA1 KO mice compared to WT and TRPV1 KO mice, but mechanical thresholds were not different between TRPV1 KO and WT mice (**Figure 8 a**). No changes in mechanical thresholds were noticed in non-treated contralateral paws (**Figure 8 b**) (Oehler et al., 2017a).

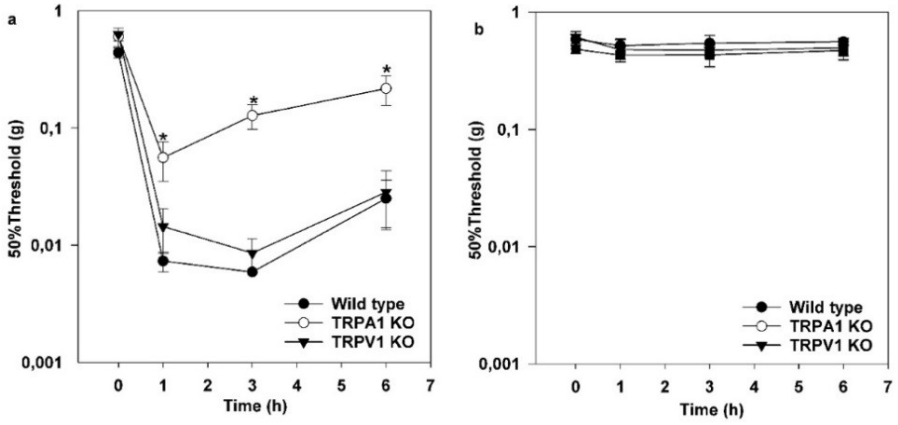

Figure 8 Reduced OxPAPC-induced tactile hypersensitivity in TRPA1 KO but not TRPV1 KO mice

50% tactile thresholds decrease after injection of 100 µg OxPAPC into TRPA1 KO, TRPV1 KO and WT mice hind paw. TRPA1 KO mice show a decreased attenuation in tactile thresholds in comparison to TRPV1 KO and WT mice (a). There is no change in contralateral paw thresholds (b). N = 6/group, *p < 0.05 versus TRPV1 KO and WT, Kruskal-Wallis ANOVA post hoc Student-Newman-Keuls).

To further elucidate the role of TRPA1 and TRPV1 ion channels in OxPAPC-induced thermal hypersensitivity, TRPA1 KO, TRPV1 KO and WT littermates were intraplantarly injected with 100 µg OxPAPC in 50 µl saline. Thermal thresholds were recorded as PWL before injections (baseline) as well as 1, 3 and 6 h after the injection. OxPAPC elicited thermal hypersensitivity only in TRPA1 KO and WT mice after injection. Thermal thresholds were significantly higher in TRPV1 KO mice at baseline and were non-respondent to OxPAPC treatment. Thermal thresholds were not different between TRPA1 KO and WT mice (**Figure 9 a**). No alteration of PWL thresholds were noticed in non-treated contralateral paws (**Figure 9 b**) (Oehler et al., 2017a).

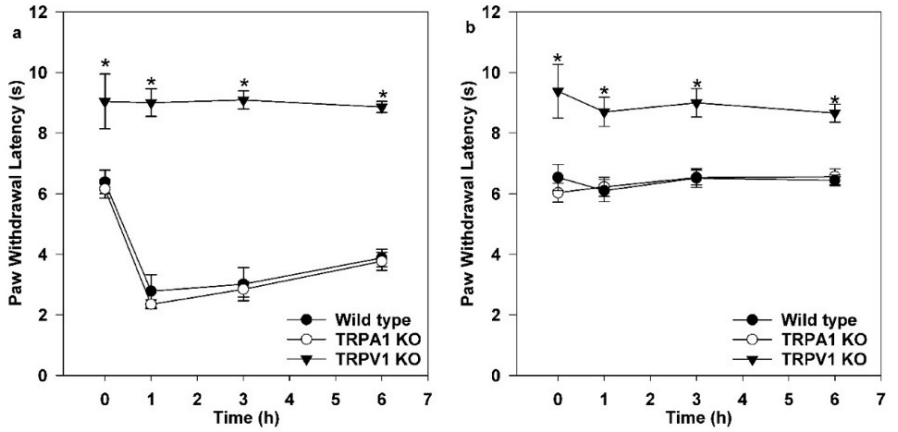

Figure 9 Normal OxPAPC-induced thermal hypersensitivity in TRPA1 KO mice

Intraplantar injection of 100 µg OxPAPC into TRPA1 KO and WT mice hind paw leads to thermal hypersensitivity with no effects on TRPV1 KO animals (a). Contralateral paw PWLs remain unaffected (b). Paw withdrawal latencies were recorded before injection (baseline) and 1 h, 3 h and 6 h after injections. Data is shown as mean paw withdrawal latency for each treatment group +/- SEM. N = 6/group, Two-way RM ANOVA, post-hoc Holm-Sidak, *p < 0.05 versus TRPA1 KO and WT mice within time point.

3.1.6 HC-030031, a TRPA1 blocker, reverses OxPAPC-induced mechanical hypersensitivity and edema

After proving that TRPA1 KO mice show a decreased level of OxPAPC-induced mechanical hypersensitivity, I asked whether pharmacological blocking TRPA1 receptors in male Wistar rats would reverse established mechanical hypersensitivity 3 h after OxPAPC injection. Baseline PPT was recorded and then 500 µg OxPAPC re-suspended in 100 µl was injected intraplantarly into rats' hind paw. PPT was once more measured 2 h and 30 min after the injection to show that mechanical thresholds are reduced and mechanical hypersensitivity is established. Under brief anesthesia, 30 mg/kg HC-030031 dissolved in 1.2 ml DMSO was intraperitoneally injected to 6 rats, 3 other rats received vehicle as control group. Half-hour after the second treatment (3 h after OxPAPC injections) PPT was measured. HC-030031 significantly reversed OxPAPC-induced mechanical hypersensitivity (**Figure 10 a**), while mechanical thresholds in vehicle group as well as contralateral paws of both groups increased slightly (**Figure 10 a, b**). PPT returned to baseline values in all groups 6 h after OxPAPC injections.

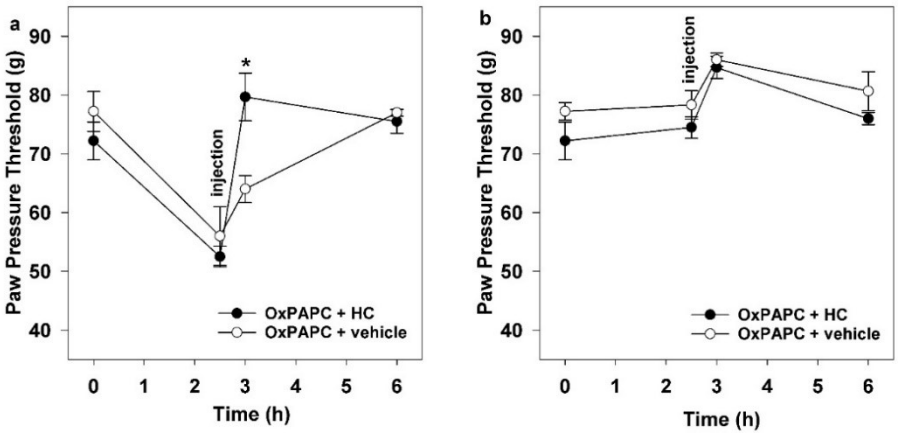

Figure 10 Reversal of OxPAPC-induced mechanical hypersensitivity by systemic injection of TRPA1 antagonist HC-030031

Intraplantar injection of 500 µg OxPAPC into rats' hind paw develops mechanical hypersensitivity 2.5 h after the injection. Intraperitoneal injection of TRPA1 antagonist HC-030031 (30 mg/kg) but not the vehicle reverses OxPAPC-induced mechanical hypersensitivity (**a**). Paw pressure thresholds on the contralateral paws does not changes significantly over time (**b**). Paw pressure thresholds were recorded before injection (baseline) and 2.5 h, 3 h and 6 h after OxPAPC injections. Data is shown as mean paw pressure thresholds for each treatment group +/- SEM. N = 6 for HC-030031 and N = 3 for vehicle group, Two-way RM ANOVA, post-hoc Holm-Sidak, *p < 0.05 versus vehicle within time point.

After knowing that application of TRPA1 antagonist reverses the mechanical hypersensitivity induced by OxPAPC, I asked whether blocking TRPA1 receptors in swollen hind paws of male Wistar rats would reverse established edema 3 h after OxPAPC injection. Baseline paw volume was recorded and then 500 µg OxPAPC resuspended in 100 µl saline was injected intraplantarly into rat hind paw. Paw volume was once more measured 2 h and 30 min after the injection to show that paws were swollen. Under brief anesthesia, 30 mg/kg HC-030031 dissolved in 1.2 ml DMSO was intraperitoneally injected to 6 rats and 3 other rats received vehicle as control group. Half-hour after

the second treatment (3 h after OxPAPC injections) paw volume was re-measured for all animals. HC-030031 significantly reversed OxPAPC-induced paw edema (**Figure 11 a**), while paw volume in vehicle group did not change significantly (**Figure 11 b**). Volumes of contralateral paws remained unchanged throughout the experiment (**Figure 11 a, b**). Volumes of the treated paws returned to baseline values in all groups 6 h after OxPAPC injections.

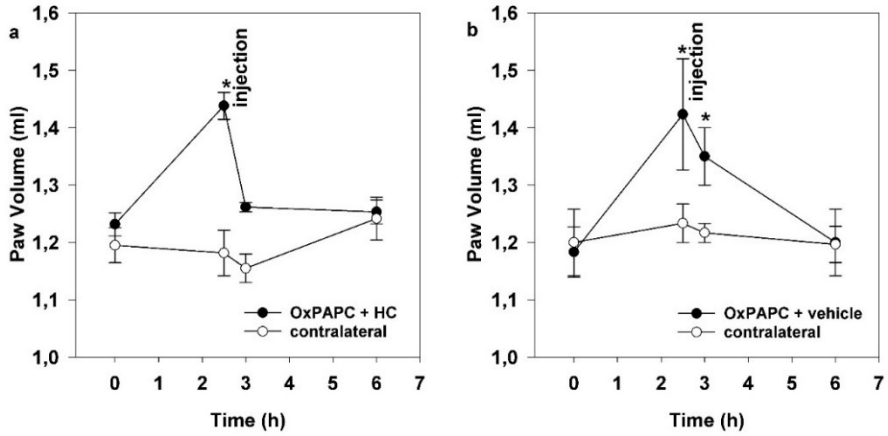

Figure 11 Reversal of OxPAPC-induced paw edema by systemic injection of TRPA1 antagonist HC-030031

Paw edema develops 2.5 h after intraplantar injection of 500 µg OxPAPC into rats' hind paw. Intraperitoneal injection of (30 mg/kg) TRPA1 antagonist HC-030031 (**a**) but not the vehicle (**b**) reverses OxPAPC-induced paw edema. Paw volume on the contralateral paws does not changes significantly over time. Paw volumes were recorded before injection (baseline) and 2.5 h, 3 h and 6 h after OxPAPC injections. Data is shown as mean paw volumes for each treatment group +/- SEM. N = 6 for HC-030031 and N = 3 for vehicle group, Two-way RM ANO, post-hoc Holm-Sidak, *p < 0.05 versus contralateral.

3.1.7 $Na_V1.9$ does not play a major role in transducing OxPAPC induced tactile and thermal hypersensitivity

To study the role of $Na_V1.9$ channels in OxPLs-induced hypersensitivity I injected a low dose (30 µg) and a high dose (100 µg) of synthetic OxPAPC in 50 µl saline in hind paws of WT and $Na_V1.9$ KO mice. The contralateral paws received the same volume of saline. Thermal and tactile thresholds were measured at baseline (0), 1, 3, and 6 h after the injections.

As shown in **Figure 12** and **Figure 13**, low dose (30 µg) and high dose (100 µg) OxPAPC induced mechanical (**a**) and thermal (**b**) hypersensitivity that maximized 1 h after injection and slowly reversed afterwards. There is no difference between $Na_V1.9$ KO and WT mice and no considerable changes in contralateral thresholds are visible.

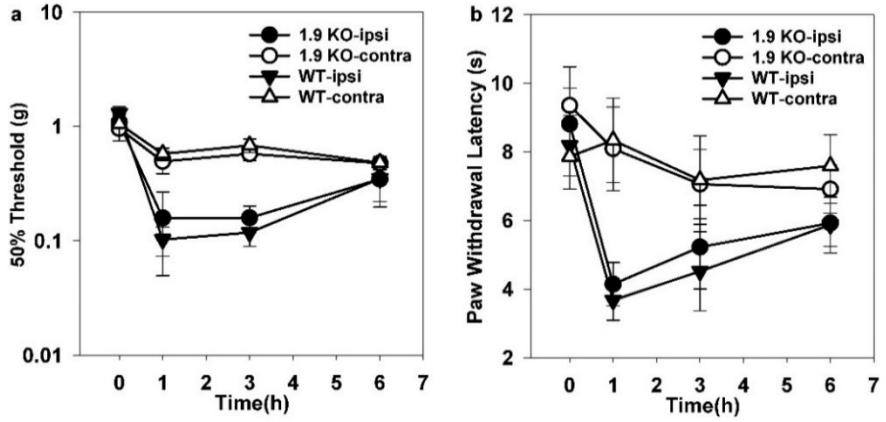

Figure 12 Low dose OxPAPC-induced thermal and tactile hypersensitivity in Nav1.9 KO as well as WT mice

Intraplantar injection of 30 µg OxPAPC into $Na_v1.9$ KO and WT mice hind paw leads to mechanical (**a**) and thermal (**b**) hypersensitivity with no differences between WT and KO animals. Contralateral paw thresholds remain unaffected. Paw withdrawal latencies and 50% tactile thresholds were recorded before injection (baseline) and 1 h, 3 h and 6 h after injections. Data is shown as mean paw withdrawal latency and 50% tactile thresholds for each treatment group +/- SEM. N = 6/group, Two-way RM ANOVA and Kruskal-Wallis ANOVA.

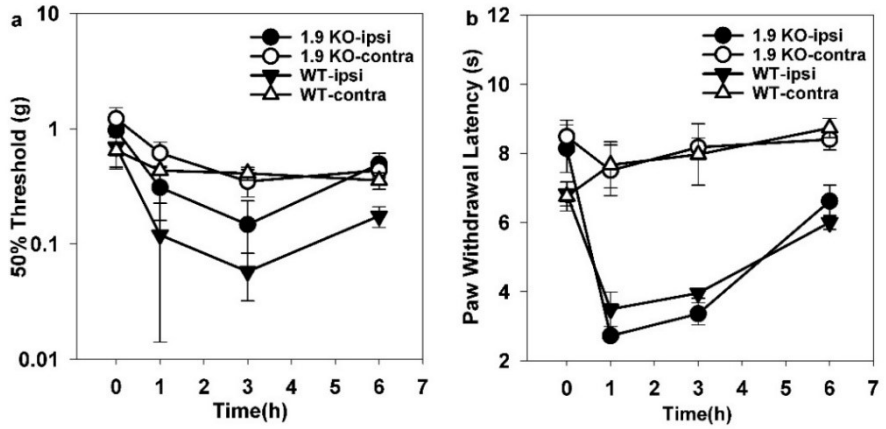

Figure 13 High dose OxPAPC-induced thermal and tactile hypersensitivity in Nav1.9 KO as well as WT mice

Intraplantar injection of 100 µg OxPAPC into $Na_v1.9$ KO and WT mice hind paw leads to mechanical (**a**) and thermal (**b**) hypersensitivity with no differences between WT and KO animals. Contralateral paw thresholds remain unaffected. Paw withdrawal latencies and 50% tactile thresholds were recorded before injection (baseline) and 1 h, 3 h and 6 h after injections. Data is shown as mean paw withdrawal latency and 50% tactile thresholds for each treatment group +/- SEM. N = 6/group, Two-way RM ANOVA and Kruskal-Wallis ANOVA.

3.2 CFA model of inflammatory pain, some of its characteristics and different approaches to alleviate pain

3.2.1 Infiltration of immune cells to CFA-induced inflamed rat paw

Infiltration of immune cells such as neutrophils and macrophages, contributes to the promotion of inflammation and production of ROS at the site of the inflammation (Hackel et al., 2013). Here, by using immunohistochemistry, I visualized the granulocytes (**Figure 14**) and macrophages (**Figure 15**) 96 h after CFA injection.

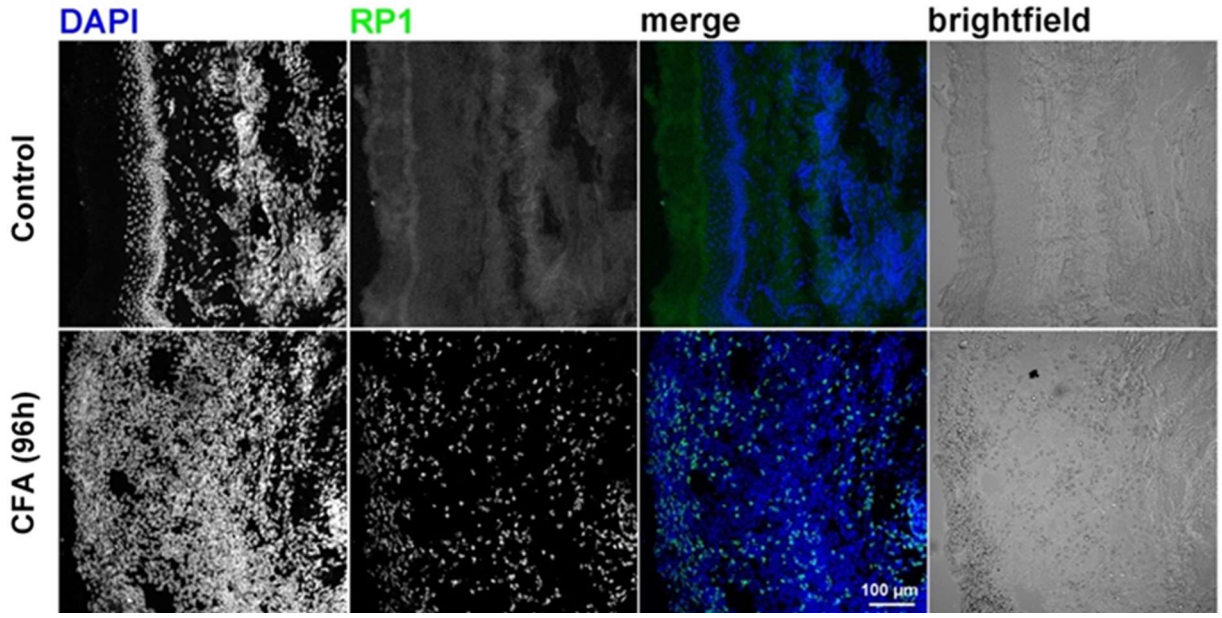

Figure 14 Representative Immunohistochemical staining of granulocyte infiltration into inflamed rat paw

Male Wistar rats were intraplantarly injected with 150 µl CFA into the ipsilateral hind paw. Ipsilateral and contralateral (as control) paw soft tissue was dissected 96 h after the injection and was fixed in 4%PFA and 30% sucrose. Serial sections were made and the slides were labeled with RP-1 mAb (1/600) against rat granulocytes, and Cy3® anti-Mouse IgG (H+L) F (ab) Fragment (1:600) and DAPI.

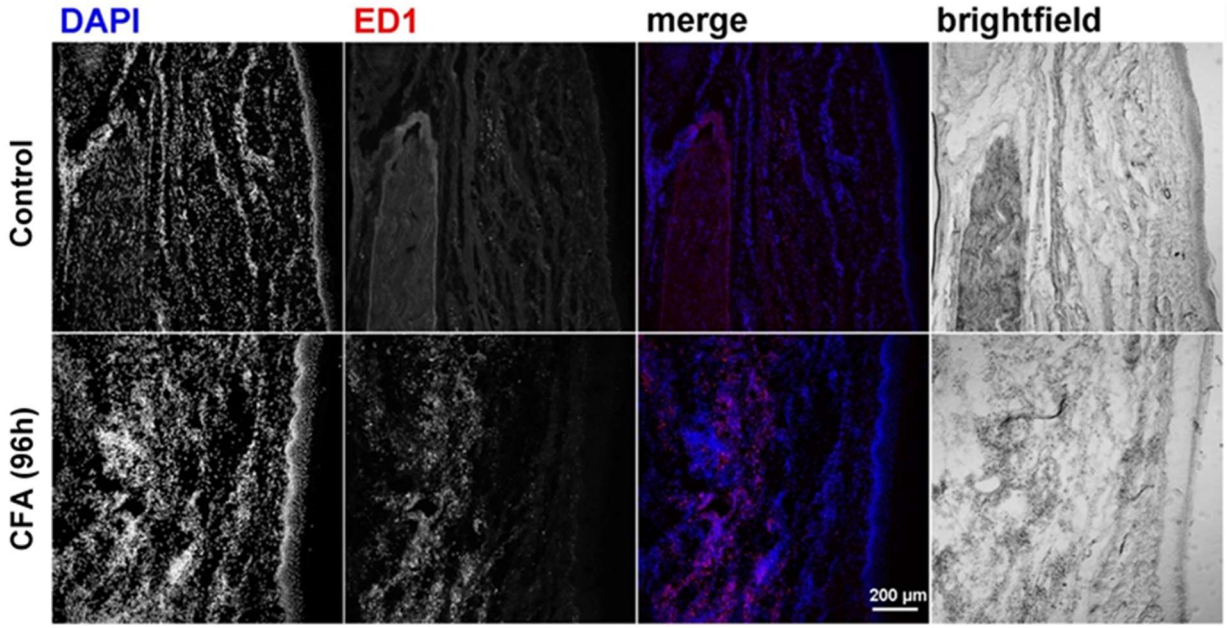

Figure 15 Representative Immunohistochemical staining of macrophage infiltration into inflamed rat paw

Male Wistar rats were intraplantarly injected with 150 µl CFA into the ipsilateral hind paw. Ipsilateral and contralateral (as control) paw soft tissue was dissected 96 h after the injection and was fixed in 4%PFA and 30% sucrose. Serial sections were made and the slides were labeled with ED-1 mAb (1/600) against rat macrophages, Cy3® Anti-Mouse IgG (H+L) F (ab) Fragment (1:600) and DAPI.

3.2.2 Accumulation of OxPLs in CFA-treated rats' paw

Extracted lipids from the rats' paw tissues were analyzed by custom-designed binding assay 3 h after 150 µl CFA injection and immidiately after 500 µg OxPAPC injection in comparison to contralateral paws with no treatments (Oehler et al., 2017a).

As shown in **Figure 16**, there is an accumulation of OxPLs 3 h after CFA treatment in rats hind paw in comparison to contraletral paws

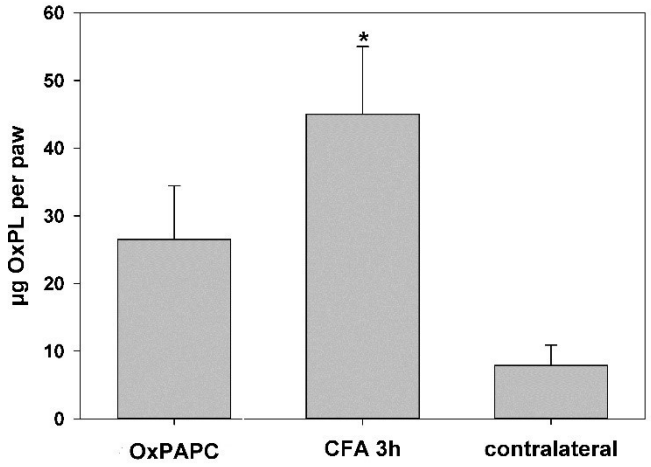

Figure 16 Accumulation of OxPLs in CFA-treated rats' inflamed paw

Male Wistar rats were intraplantarly treated with either OxPAPC (500 µg) or CFA (150 µl), then lipids were extracted from the paw *ex vivo* after 3 h for CFA and immediately after injection for OxPAPC treatments. Using a competitive binding assay, there are significantly more E06 mAb reactive lipids in rat paws 3 h after CFA treatment in comparison to contralateral paws. Data is shown as mean amount of E06 mAb-reactive lipids per paw +/- SEM. OxPAPC (N = 6), CFA (N = 6), contralateral (N = 5), One-way ANOVA, post-hoc Holm-Sidak, *p < 0.05 compared to contralateral.

3.2.3 E06 prevents development of CFA-induced mechanical but not thermal hypersensitivity

To examine the potential of E06 mAb in blocking development of inflammatory hypersensitivity, different doses of E06 mAb or IgM isotype control were co-injected with CFA then mechanical and thermal thresholds were recorded. As shown in **Figure 17 (a and b),** E06 mAb prevents development of mechanical inflammatory hypersensitivity but has no effects on thermal inflammatory hypersensitivity (**Figure 17 c and d**) (Oehler et al., 2017a).

.

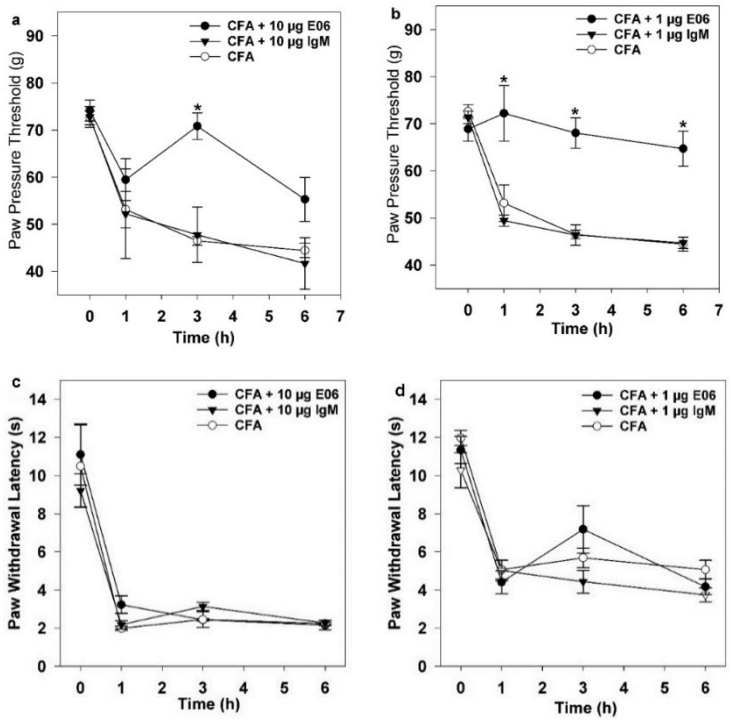

Figure 17 Prevention of CFA-induced mechanical hypersensitivity and no effects on thermal hypersensitivity by E06 mAb

Intraplantar injection of 150 µl CFA leads to mechanical and thermal inflammatory hypersensitivity. Mechanical inflammatory hypersensitivity is prevented by either 10 µg (**a**) or 1 µg (**b**) E06 mAb while Intraplantar co-injection of either 10 µg (**c**) or 1 µg (**d**) E06 mAb has no effect on thermal inflammatory hypersensitivity. In contrast, 10 µg or 1 µg IgM isotype has no effects on paw withdrawal latencies and paw pressure thresholds. Paw withdrawal latencies and paw pressure thresholds were recorded before injection (baseline) and 1 h, 3 h and 6 h after injections. Data is shown as mean paw withdrawal latencies and paw pressure thresholds for each treatment group +/- SEM. N = 6/group, Two-way RM ANOVA, post-hoc Holm-Sidak, *p < 0.05 versus IgM isotype or saline within time point.

3.2.4 E06 reverses CFA-induced mechanical hypersensitivity

To evaluate the efficacy of E06 mAb to reverse a well-established inflammatory mechanical hypersensitivity, 1 µg E06 mAb was intraplantarly injected into rats' hind paw 3 h after CFA injection. As shown in **Figure 18** E06 mAb reversed an established mechanical hypersensitivity (Oehler et al., 2017a).

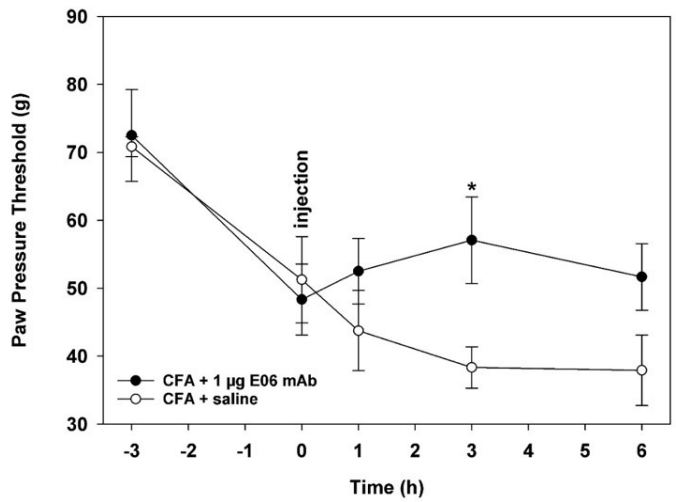

Figure 18 Reversal of CFA-induced mechanical hypersensitivity by E06 mAb

Intraplantar injection of 150 µl CFA leads to mechanical inflammatory hypersensitivity 3 h after injection that could be reversed by 1 µg E06 mAb. Paw pressure thresholds were recorded before injection (baseline) and 3 h, 4 h, 6h and 9 h after injections. Data is shown as mean paw pressure thresholds for each treatment group +/- SEM. N = 4/group, Two-way RM ANOVA, post-hoc Holm-Sidak, *p < 0.05 versus saline within time point.

3.3 **E06 mAb and D-4F peptide induced amelioration of prolonged mechanical hypersensitivity induced by TRPA1/V1 agonists**

E06 mAb and D-4F peptide bind OxPLs and prevents or reverses mechanical hypersensitivity after local OxPAPC injection and in CFA-induced inflammatory pain (Oehler et al., 2017b). I now wanted to delineate which other proalgesic effects of molecules from the ROS pathway and metabolism are blocked by E06 mAb. To this end, I evaluated ROS-sources like H_2O_2 and the downstream lipid peroxidation metabolite 4-HNE. As controls the TRPA1 and TRPV1 agonists, AITC and capsaicin respectively, were chosen. E06 mAb, isotype control Ab or saline on one hand and D-4F peptide and saline on the other hand were intraplantarly co-injected with the aforementioned agonists (**Figure 19** and **Figure 20**). Paw pressure thresholds decreased after 4-HNE injection and reached their minimum 3 h after injection in control groups treated with saline and IgM isotype group. E06 mAb and D-4F peptide significantly attenuated 4-HNE-induced mechanical hypersensitivity (**Figure 19 a** and **Figure 20 a**). Similarly, intraplantar injection of H_2O_2 led to mechanical hypersensitivity with the lowest mechanical nociceptive threshold after 3 h. However, E06 mAb did not change nociceptive thresholds in comparison to the control groups (**Figure 19 b**) while D-4F peptide blocked the development of H_2O_2-induced mechanical hypersensitivity (**Figure 20 b**). Intraplantar AITC injection caused mechanical hypersensitivity, peaked at 3-6 h after the injection. This was significantly prevented by E06 mAb and D-4F peptide in comparison to control groups (**Figure 19 c** and **Figure 20 c**). A similar pattern was observed after capsaicin application: intraplantar capsaicin injection elicited mechanical hypersensitivity, which climaxed 1 h after the injection. This was blocked by E06 mAb and D-4F peptide in comparison to the controls (**Figure 19 d** and **Figure 20 d**). There were no changes in the thresholds of the contralateral paws (**Figure 19** and **Figure 20 e, f, g** and **h)** (Mohammadi *et al.*, 2018).

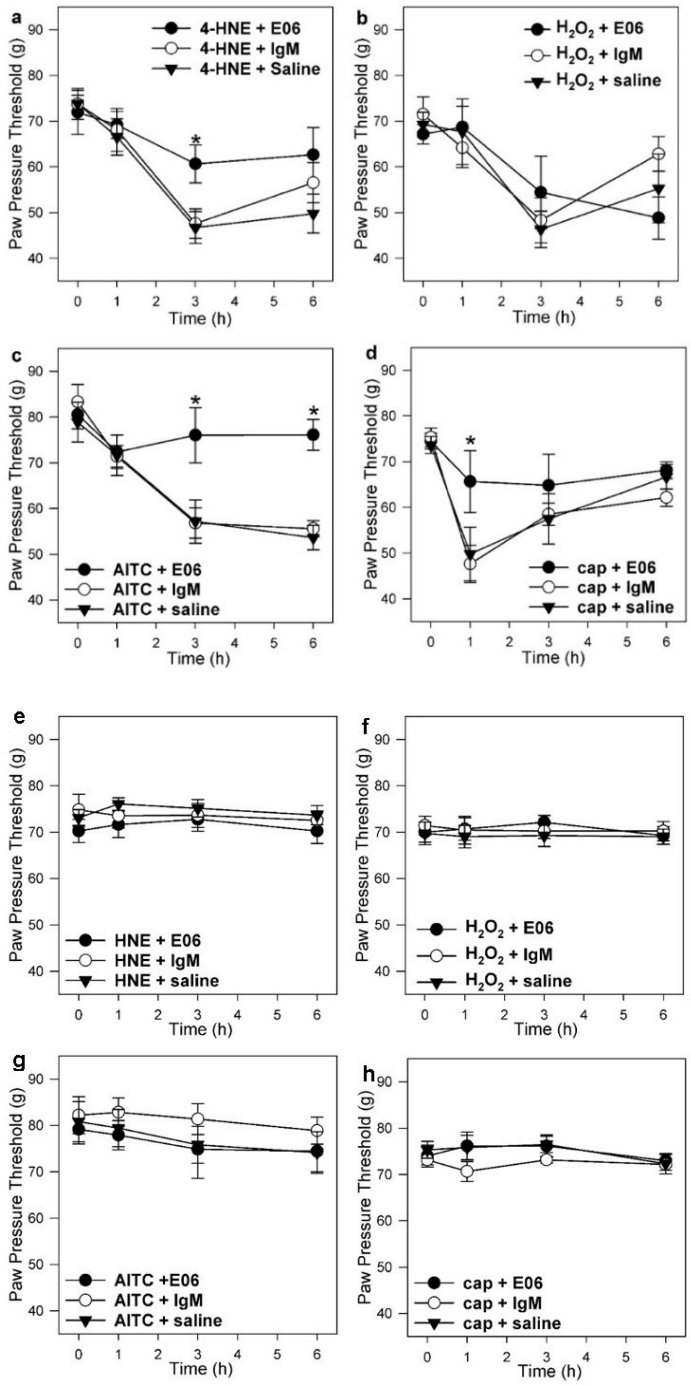

Figure 19 Sensitivity of 4-HNE, AITC and capsaicin-induced mechanical hypersensitivity to E06 mAb blockade with no changes in the mechanical thresholds of the contralateral paws

TRPA1/V1 agonists, 6 µmol 4-HNE (**a**), 19.2 µmol H_2O_2 (**b**), 10 µmol AITC (**c**) or 245 nmol capsaicin (**d**) together with E06 mAb (2 µg), IgM isotype control (2 µg) or saline were intraplantarly injected into rats' hind paw. Mechanical hypersensitivity (paw pressure thresholds) were measured before injection and 1, 3 and 6 h after injection. Mechanical thresholds remain unchanged in the contralateral hind paw of male Wistar rats after co-injection of either 2 µg E06 mAb, 2 µg IgM isotype or saline with 6 µmol 4-HNE (**e**), 19.2 µmol H_2O_2 (**f**), 10 µmol AITC (**g**) or 245 nmol capsaicin (**h**) into the ipsilateral paw. Data is shown as mean+/- SEM. 4-HNE (N = 6), H_2O_2 (N = 7), AITC (N = 6), capsaicin (N = 6), Two-way RM ANOVA, post-hoc Holm-Sidak, *p < 0.05 versus IgM isotype or saline

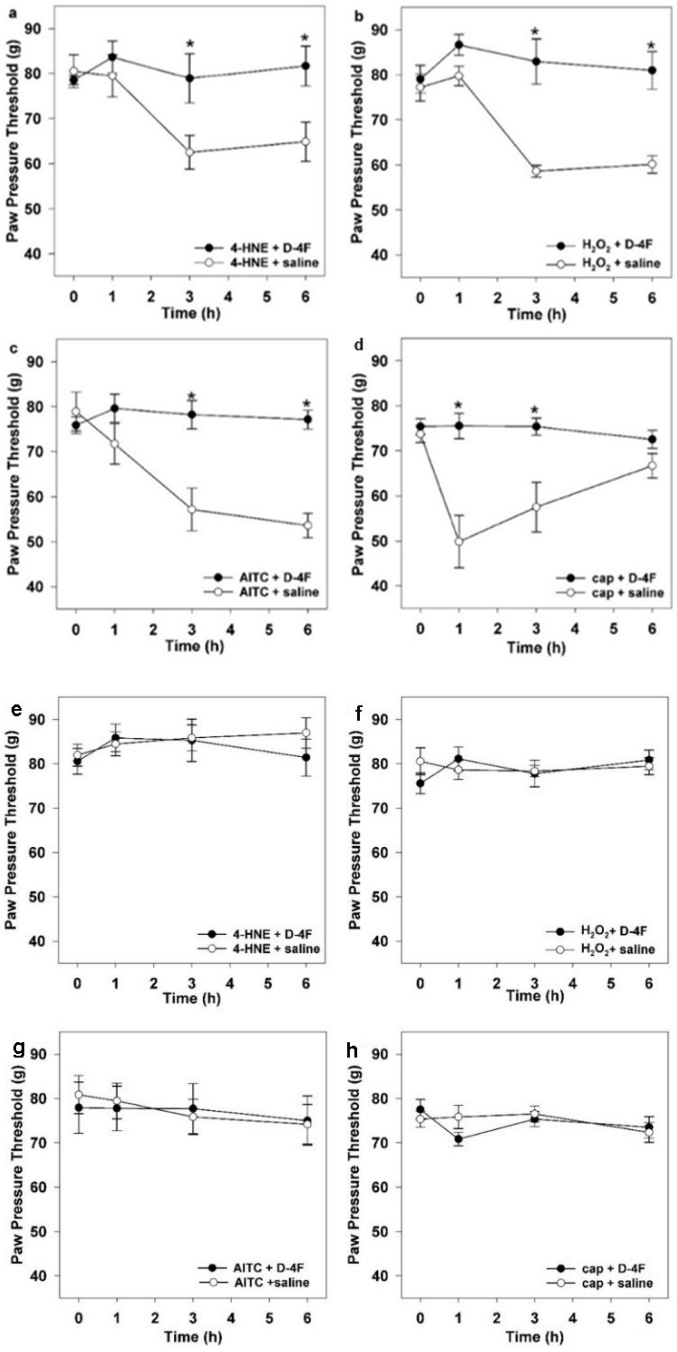

Figure 20 Prevention of mechanical hypersensitivity induced by TRPA1/V1 agonists and no changes in the mechanical thresholds of the contralateral paws by D-4F peptide

Male Wistar rats were intraplantarly injected with either 6 µmol 4-HNE (**a**), 19.2 µmol H_2O_2 (**b**), 10 µmol AITC (**c**) or 245 nmol capsaicin (**d**) together with D-4F peptide (500 µg) or saline. Mechanical thresholds remain unchanged in the contralateral hind paw of male Wistar rats after co-injection of either D-4F peptide (500 µg) or saline with 6 µmol 4-HNE (**e**), 19.2 µmol H_2O_2 (**f**), 10 µmol AITC (**g**) or 245 nmol capsaicin (**h**) into the ipsilateral paw. Mechanical hypersensitivity (paw pressure thresholds) were measured before injection and 1, 3 and 6 h after injection. Data is shown as mean+/- SEM. 4-HNE (N = 6) H_2O_2 (N = 6), AITC (N = 8), capsaicin (N = 6), Two-way RM ANOVA, post-hoc Holm-Sidak, *p < 0.05 versus IgM isotype or saline.

3.4 No effects of E06 mAb on prolonged thermal hypersensitivity induced by TRPA1/V1 agonist

Intraplantar injection of 4-HNE, H_2O_2, AITC and capsaicin also resulted in thermal hypersensitivity with a maximum at 3-6 h after 4-HNE, H_2O_2, AITC or 1 h for capsaicin (**Figure 21**). Co-injection of E06 mAb, however, had no effect on development or severity of thermal hypersensitivity. In all of the experiments, thermal withdrawal reflex thresholds did not change in the contralateral paws (**Figure 23** and **Figure 24**). In contrary, co-injection of D-4F peptide blocked development of 4-HNE and capsaicin-induced thermal hypersensitivity (**Figure 22**) (Mohammadi *et al.*, 2018).

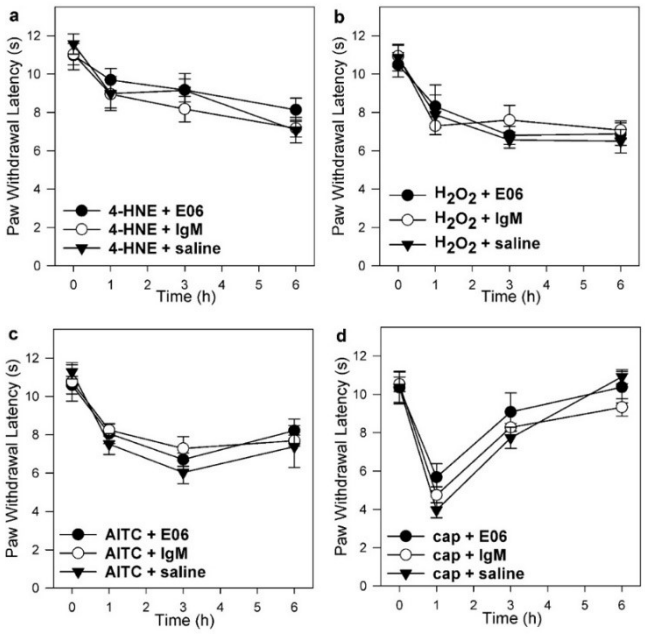

Figure 21 Unaltered 4-HNE, H2O2, AITC or capsaicin-induced thermal hypersensitivity after E06 mAb treatment

Thermal hypersensitivity as paw withdrawal latency was measured in male Wistar rats after intraplantar co-application of either 2 µg E06 mAb, 2 µg IgM isotype or saline with 6 µmol 4-HNE (**a**), 19.2 µmol H_2O_2 (**b**), 10 µmol AITC (**c**) or 245 nmol capsaicin (**d**) in separate injections. Paw withdrawal latencies were recorded before injection (baseline) and 1 h, 3 h and 6 h after injections. Data is shown as mean paw withdrawal latency for each treatment group +/- SEM. N = 6/group, Two-way RM ANOVA, $p > 0.05$.

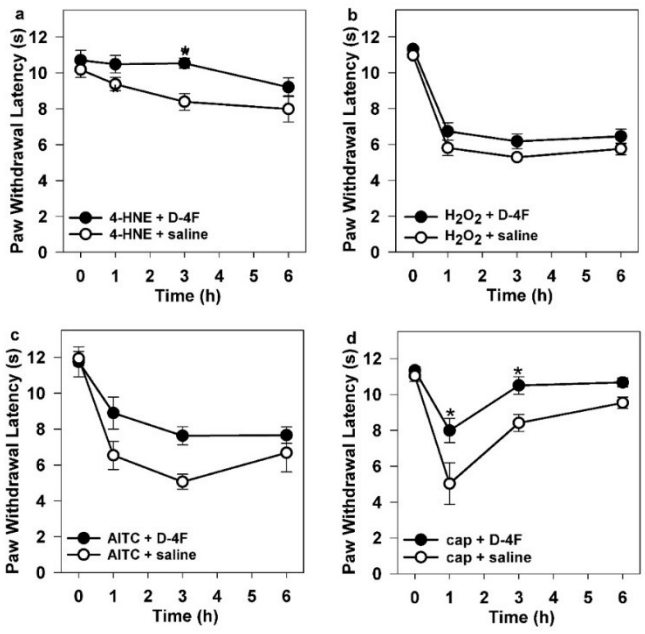

Figure 22 Attenuation of thermal hypersensitivity induced by capsaicin and 4-HNE by D-4F peptide

Thermal hypersensitivity as paw withdrawal latency was measured in male Wistar rats after intraplantar co-application of either 500 µg D-4F peptide or saline with 6 µmol 4-HNE (**a**), 19.2 µmol H_2O_2 (**b**), 10 µmol AITC (**c**) or 245 nmol capsaicin (**d**) in separate injections. Paw withdrawal latencies were recorded before injection (baseline) and 1 h, 3 h and 6 h after injections. Data is shown as mean paw withdrawal latency for each treatment group +/- SEM. N = 6-7/group, Two-way RM ANOVA, * $p < 0.05$.

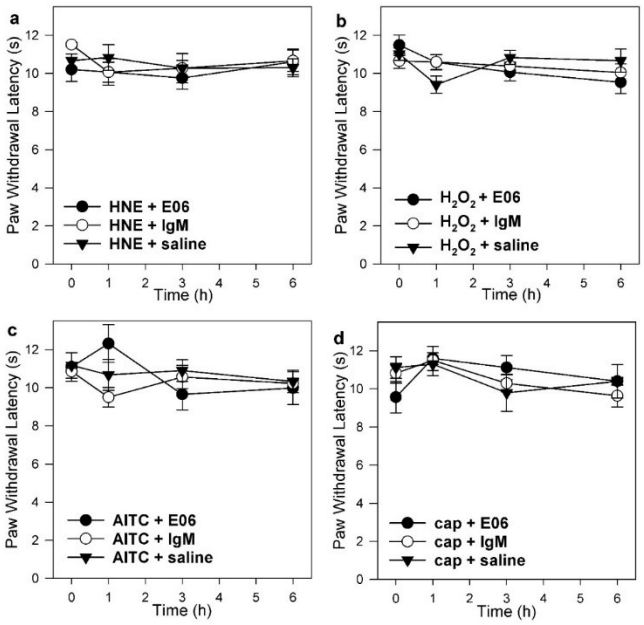

Figure 23 No effects on thermal thresholds of the contralateral paws after TRPA1/V1 agonist treatment

Thermal thresholds remain unchanged in the contralateral hind paw of male Wistar rats after co-injection of either 2 µg E06 mAb, 2 µg IgM isotype or saline with 6 µmol 4-HNE (**a**), 19.2 µmol H_2O_2 (**b**), 10 µmol AITC (**c**) or 245 nmol capsaicin (**d**) into the ipsilateral paw. Paw withdrawal latencies were recorded before injection (baseline) and 1 h, 3 h and 6 h after injections. Data is shown as mean paw withdrawal latency for each treatment group +/- SEM. 4-HNE (N = 6), H_2O_2 (N = 6), AITC + E06 (N = 6), AITC + IgM (N = 5), AITC + saline (N = 5), capsaicin (N = 6), Two-way RM ANOVA, $p > 0.05$.

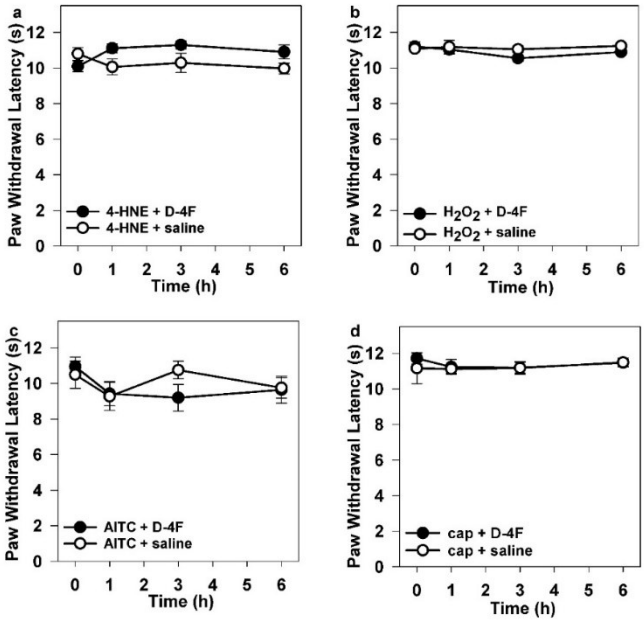

Figure 24 No changes in thermal thresholds of the contralateral paws after TRPA1/V1 agonist treatment

Thermal thresholds remain unchanged in the contralateral hind paw of male Wistar rats after co-injection of either 500 µg D-4F peptide or saline with 6 µmol 4-HNE (**a**), 19.2 µmol H_2O_2 (**b**), 10 µmol AITC (**c**) or 245 nmol capsaicin (**d**) into the ipsilateral paw. Paw withdrawal latencies were recorded before injection (baseline) and 1 h, 3 h and 6 h after injections. Data is shown as mean paw withdrawal latency for each treatment group +/- SEM. N = 6-7/group, Two-way RM ANOVA, $p > 0.05$.

3.4.1 Acute hypersensitivity after intraplantar injection of D-4F peptide

To test the effects of D-4F peptide on acute nociception, first I compared spontaneous nocifensive and affective-motivational responses induced by injection of 500 µg D-4F to saline. As shown in **Figure 25**, injection of D-4F peptide leads to significant increase in spontaneous nocifensive and affective-motivational responses. Therefore, the possible blocking effects of D-4F on spontaneous nocifensive and affective-motivational behaviors induced by the aforementioned irritants could not be investigated.

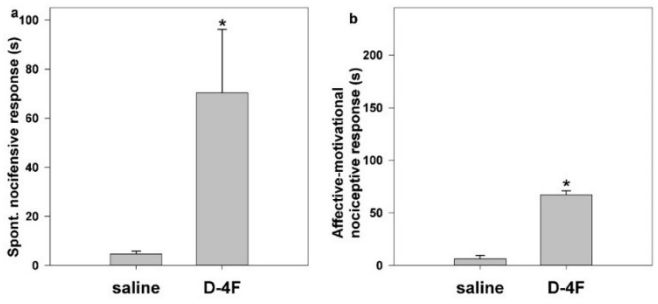

Figure 25 Spontaneous nocifensive and affective-motivational nociceptive responses induced by D-4F peptide

Duration of spontaneous nocifensive (**a**) and affective-motivational (**b**) behavior in male Wistar rats were recorded after intraplantar administration of either 500 µg D-4F peptide or saline. Data is shown as mean cumulative duration of spontaneous nocifensive or affective-motivational behavior within 10 min after injection for each treatment group +/- SEM. N = 3 per group, student t-test, *p < 0.05.

3.4.2 D-4F peptide potentiates capsaicin-induced paw edema

To check the possible antiedemic effects of D-4F peptide, it was co-injected with capsaicin. As expected, capsaicin 1 h after injection induced edema in rats' hind paw but surprisingly, co-injection of D-4F peptide not only did not block capsaicin-induced paw edema but potentiated the swelling significantly (**Figure 26 a**). Volume of the contralateral paws did not change over the time (**Figure 26 b**).

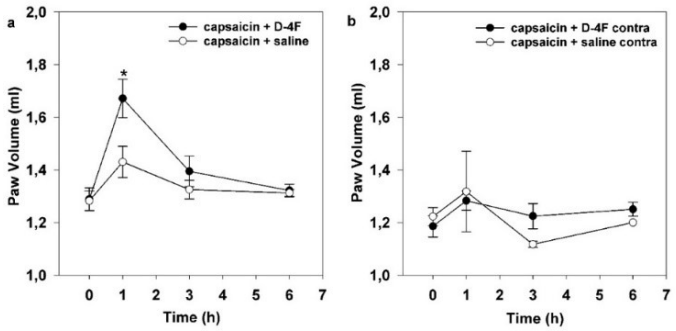

Figure 26 D-4F-induced enhanced edema in capsaicin-treated rat hind paw

Intraplantar co-injection of 500 µg D-4F peptide with 245 nmol capsaicin into rats' hind paw potentiates capsaicin-induced paw edema 1 h after injection (**a**). Paw volume on the contralateral paws does not changes significantly over time (**b**). Paw volumes were recorded before injection (baseline) and 1 h, 3 h and 6 h after injections. Data is shown as mean paw volumes for each treatment group +/- SEM. N = 4 for saline and N = 7 for D-4F peptide group, Two-way RM ANOVA, post-hoc Holm-Sidak, *p < 0.05 versus vehicle within time point.

3.4.3 Lack of E06-mediated blockage of acute nociception

Local application of TRPA1 or TRPV1 agonists not only activates the respective receptors on nociceptors but also initiates an inflammatory cascade leading to neurogenic inflammation. To specifically examine the early presumably more receptor specific events, the ability of E06 mAb to block the acute spontaneous nocifensive behavior and affective-motivational behavior immediately

after injection of 4-HNE, H_2O_2, AITC and capsaicin was assessed. Injection of E06 mAb, IgM isotype or saline did not elicit considerable nocifensive behaviors *per se* (**Figure 27**). All agonists elicited affective-motivational (**Figure 28**) and spontaneous nocifensive (**Figure 29**) behavior with a distinctive magnitude in comparison to control treatments.

To mimic the calcium imaging experiments, agonists were pre-incubated with E06 mAb, IgM isotype or the vehicle before intraplantar injection. Neither affective-motivational nociceptive behaviors (**Figure 28**) nor spontaneous nocifensive responses (**Figure 29**) were modulated by E06 co-incubation. In summary, in the immediate phase of hypersensitivity, E06 mAb does not prevent nocifensive behavior or affective-motivational behavior (Mohammadi *et al.*, 2018).

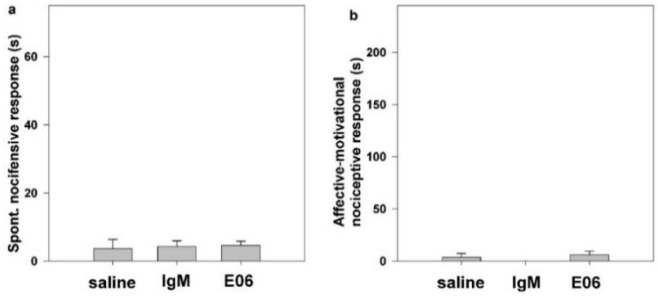

Figure 27 No prominent nociceptive behavior by intraplantar injection of E06 mAb or IgM isotype in comparison to saline

Duration of spontaneous nocifensive behavior (**a**) and Affective-motivational behavior (**b**) following intraplantar injection of either saline, 2 µg IgM isotype or 2 µg E06 mAb into rats' hind paw was measured. Data is shown as mean cumulative duration of behavior within 10 min after injection for each treatment group +/- SEM. N = 3/group.

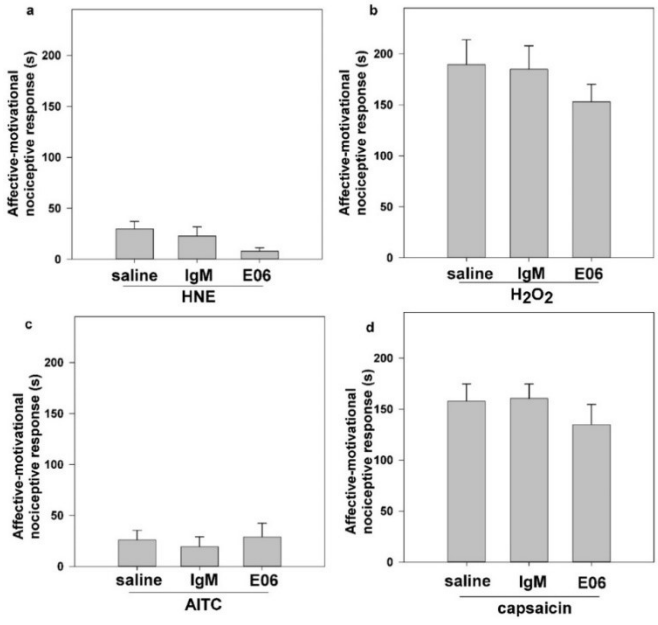

Figure 28 Lack of E06 mAb-induced blockade of affective-motivational behaviors due to intraplantar irritants

Affective-motivational behavior following intraplantar injection of 6 µmol 4-HNE (**a**), 19.2 µmol H_2O_2 (**b**), 10 µmol AITC (**c**) or 245 nmol capsaicin (**d**) pre-incubated with either saline, 2 µg IgM isotype or 2 µg E06 mAb into rats' hind paw was measured. Data is shown as mean cumulative duration of affective motivational behaviors within 10 min after injection for each treatment group +/- SEM. 4-HNE (N = 10), H_2O_2 (N = 7), AITC (N = 5), capsaicin (N = 5), One-way ANOVA, $p > 0.05$ compared to IgM.

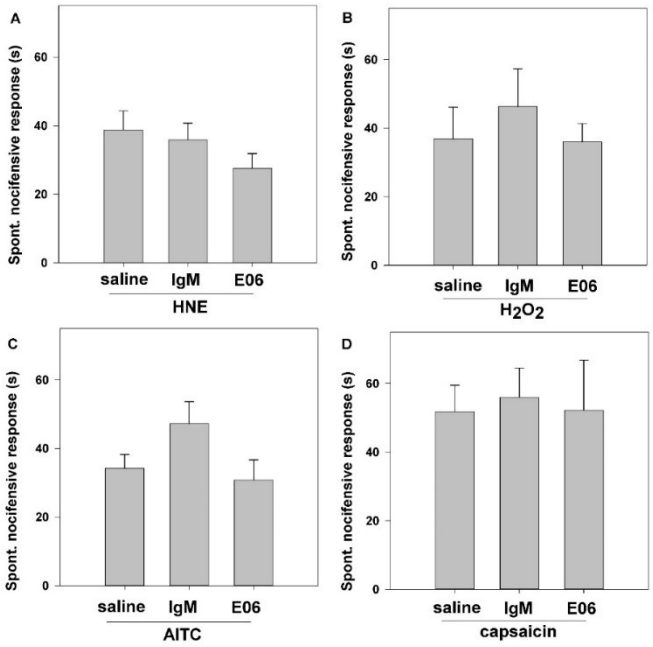

Figure 29 Resistance of pungent-induced spontaneous nocifensive behavior to E06 mAb blockade

Duration of spontaneous nocifensive behavior in male Wistar rats were recorded after intraplantar administration of 6 µmol 4-HNE (**a**), 19.2 µmol H_2O_2 (**b**), 10 µmol AITC (**c**) or 245 nmol capsaicin (**d**) pre-incubated with either saline, 2 µg E06 mAb or 2 µg IgM. Data is shown as mean cumulative duration of spontaneous nocifensive behavior within 10 min after injection for each treatment group +/- SEM. 4-HNE (N = 10), H_2O_2 (N = 7), AITC (N = 5), capsaicin (N = 5), One-way ANOVA, post-hoc Holm-Sidak, *p < 0.05.

3.4.4 No binding of E06 mAb to either 4-HNE or 4-HNE-BSA

Based on the in vivo findings, I could not rule out that E06 neutralizes 4-HNE bioactivity via immunoreactive binding. To this end, I performed a series of direct and competitive binding assays. While synthetic OxPAPC dose-dependently bound to fluorescent E06 mAb in a competitive (**Figure 30 a**) and a direct (**Figure 30 b**) assay, no binding of 4-HNE or 4-HNE protein adducts to E06 mAb was detectable (Mohammadi *et al.*, 2018).

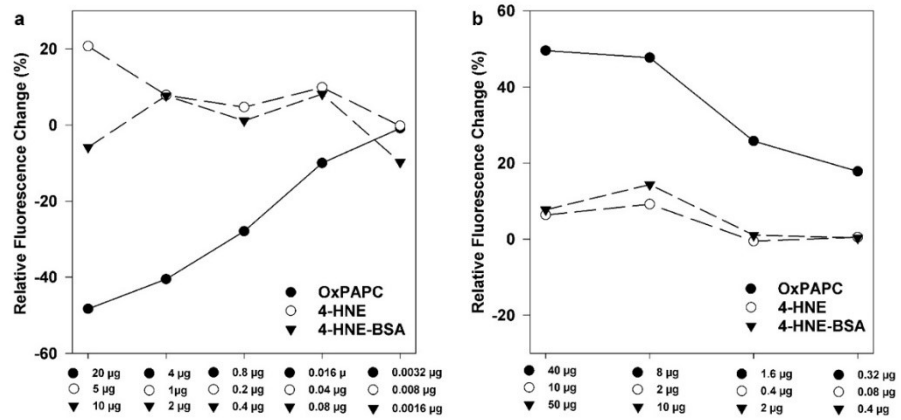

Figure 30 No in vitro binding of E06 mAb to 4-HNE or 4-HNE-BSA

4-HNE or 4-HNE coupled to BSA in different concentrations as outlined were incubated together with E06 mAb in two different binding assays. Fluorescent E06 mAb dose-dependently bound to synthetic OxPAPC as a positive control but not to 4-HNE and 4-HNE protein adduct in the competitive (**a**) and direct (**b**) binding assays. Representative graphs of 6 individual experiments are displayed.

3.4.5 Accumulation of E06-reactive phospholipids in rats' paws

Finally, I hypothesized that TRPA1 or TRPV1 activation as well as ROS metabolites stimulate the production of OSE like OxPLs. To this end, subcutaneous paw tissue was harvested at the time point with maximum hypersensitivity. Competitive binding assays showed significantly higher amounts of E06 mAb binding lipids in paws treated with H_2O_2, 4-HNE, AITC and capsaicin in comparison to saline treated rat paws (**Figure 31**). These data thus indicate that irritant-induced inflammatory reactions lead to accumulation of OxPLs (Mohammadi *et al.*, 2018).

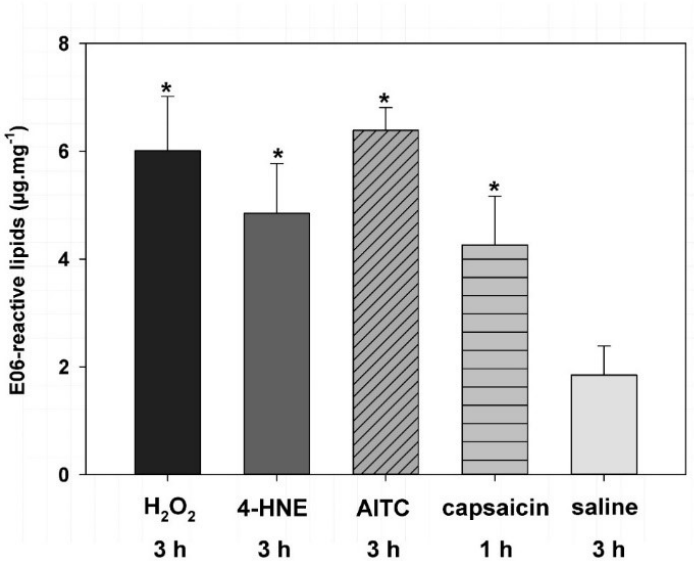

Figure 31 Accumulation of OxPLs in rat paws treated with TRPA1 and TRPV1 agonists

E06 mAb-reactive lipids from hind paws were quantified in comparison to OxPAPC. Male Wistar rats were intraplantarly treated with either H_2O_2, 4-HNE, AITC, capsaicin or saline. Lipids were extracted from the paws ex vivo after indicated time points. Using a competitive binding assay, there were significantly more E06 mAb reactive lipids in rat paws 3 h after H_2O_2, 4-HNE and AITC and 1 h after capsaicin treatment in comparison to saline treated paws. Data is shown as mean amount of E06 mAb-reactive lipids per mg of wet paw tissue +/- SEM. H_2O_2 (N = 6), 4-HNE (N = 7), AITC (N = 5), capsaicin (N = 6), saline (N = 6), One-way ANOVA, post-hoc Holm-Sidak, *p < 0.05 compared to saline.

3.5 Gait analysis as a novel non-reflexive pain measurement

CatWalk is an automated quantitative gait analysis system that uses a high throughout technology to capture rodents' gait and produce large data sets. CatWalk is capable to calculate up to 34 predefined parameters from the captured videos. This experiment was conducted on exploratory manner to evaluate the potential of CatWalk on evaluation of CFA inflammatory pain model and its predictability on assessment of analgesics and anti-hyperalgesic agents. Several gait parameters were affected by CFA inflammation:

- **Swing** or **Swing Phase** is the duration in seconds of no contact of a paw with the glass plate.
- **Max Contact Area** is the maximum area of a paw that comes into contact with the glass plate.
- **Swing speed** is the speed of the paw in the swing phase.
- **Stand Index** is defined as a measure for the speed at which the paw loses contact with the glass plate.

- **Single Stance** is the duration of ground contact for a single hind paw. It is used for gait analysis in pain models.
- **Mean intensity** is the mean intensity of the complete paw.

However, most of these changes were not reversible by either single intraplantar injections of 3 µg fentanyl or 500 µg D-4F. Stand index was the only factor that was greatly reversed in the contralateral paw after D-4F or fentanyl treatment.

Changes in swing duration: At the baseline, both the contralateral (LH) and ipsilateral (RH) paws had similar swing time before CFA injection. After CFA injection, swing duration gradually increased in ipsilateral paws while it decreased in contralateral paws. In the ipsilateral paw, after either fentanyl or saline injection, swing duration continued to decrease. Conversely, in the contralateral paw, swing duration increased after fentanyl while it slightly decreased in saline-treated group. There was no considerable difference between D-4F and saline-treated groups in either contralateral or ipsilateral paws

Changes in max contact area: In the ipsilateral paw, after CFA injection max contact area gradually decreased. This decrease continued after fentanyl injection while it remained at the same level after saline injection. In the contralateral paw, max contact area did not considerably change after CFA injection, but slightly decreased after fentanyl injection while it stayed unchanged after saline injection. D-4F or saline did not show any prominent effect.

Changes in swing speed: After CFA injection, swing speed decreased in ipsilateral paw and increased in the contralateral paws. D-4F or saline did not change the decrease trend of the swing speed in ipsilateral paws. In the contralateral paws, swing speed did not change after CFA injection but fentanyl administration decreased it prominently.

Changes in stand index: Stand index gradually decreased in the ipsilateral and increased the contralateral paws after CFA injection. Interestingly, fentanyl but not saline reversed these trends in the ipsilateral and contralateral paws while D-4F treatment reversed the trend only in the contralateral paws.

Changes in print area: CFA Inflammation severely decreased print area in the ipsilateral paw that did not recover with fentanyl or D-4F treatments. Print area slightly increased it in the contralateral paws after inflammation.

Changes in max contact mean intensity: After inflammation, max contact mean intensity decreased in the ipsilateral but not in the contralateral paws. While fentanyl decreased the max contact mean intensity in both paws, D-4F treatments had no effect on both paws. In **Figures 32-37** (**a** and **b**) these factors are shown for each treatment separately, so the time course of the effects is shown and the comparison of different timepoints is possible.

In contrary, in **Figures 32-37** (**c** and **d**) these factors are shown within each timepoint so different treatments within time points could be easily compared. Although figures (a and b) and (c and d) are using the same dataset, their different representation provides more information for the observer.

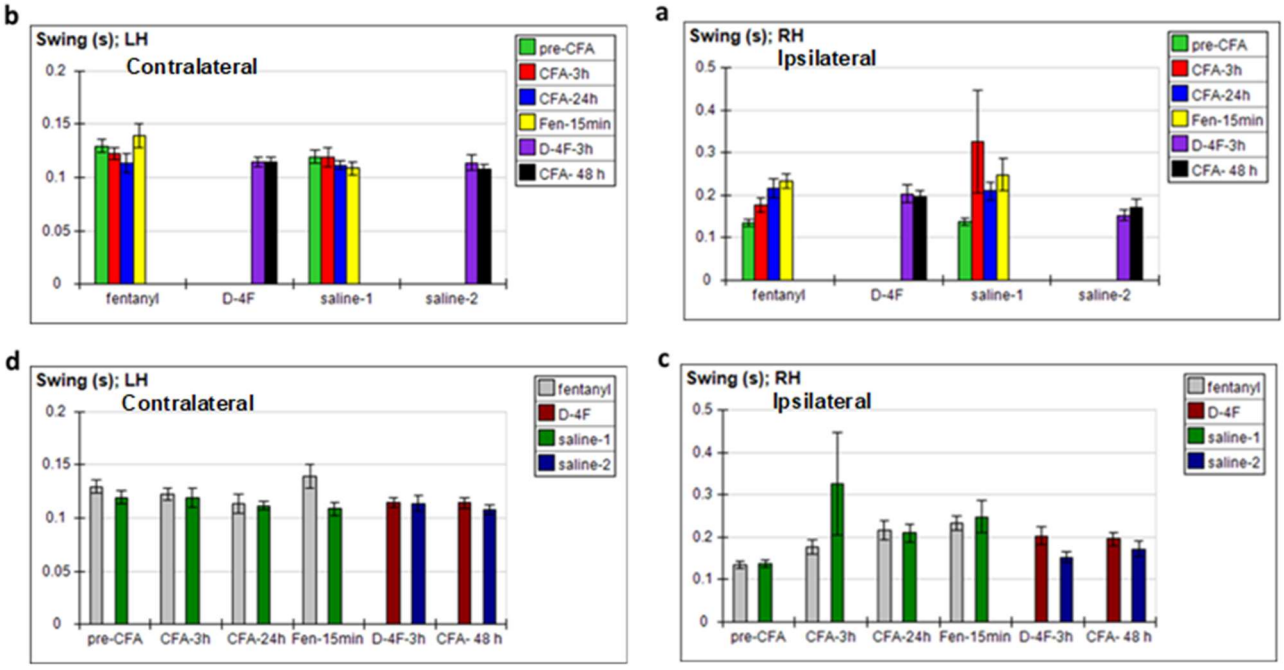

Figure 32 Effects of inflammation on swing duration of the rats' hind paw

Inflammation increased swing duration in the ipsilateral paw (**a** and **c**) and decreased it in the contralateral paws (**b** and **d**). Fentanyl treatment reversed these changes only in the contralateral paws (**b** and **d**). Male Wistar rats were injected with 150 µl CFA in the ipsilateral hind paw after the baseline recording and were recorded again 3 and 24 h after CFA injection. Then 3 µg fentanyl in 100 µl saline was injected into the ipsilateral hind paw of the experimental group and the control group received vehicle. After 15 min, the animals' gaits were recorded. Forty-eight hours after CFA treatment the gaits were recorded and then 500 µg D-4F peptide in 100 µl saline was into the ipsilateral hind paw of the experimental group and the control group received vehicle. After 3 h, gait behavior was recorded for the last time then animals were euthanized. N = 6 per group

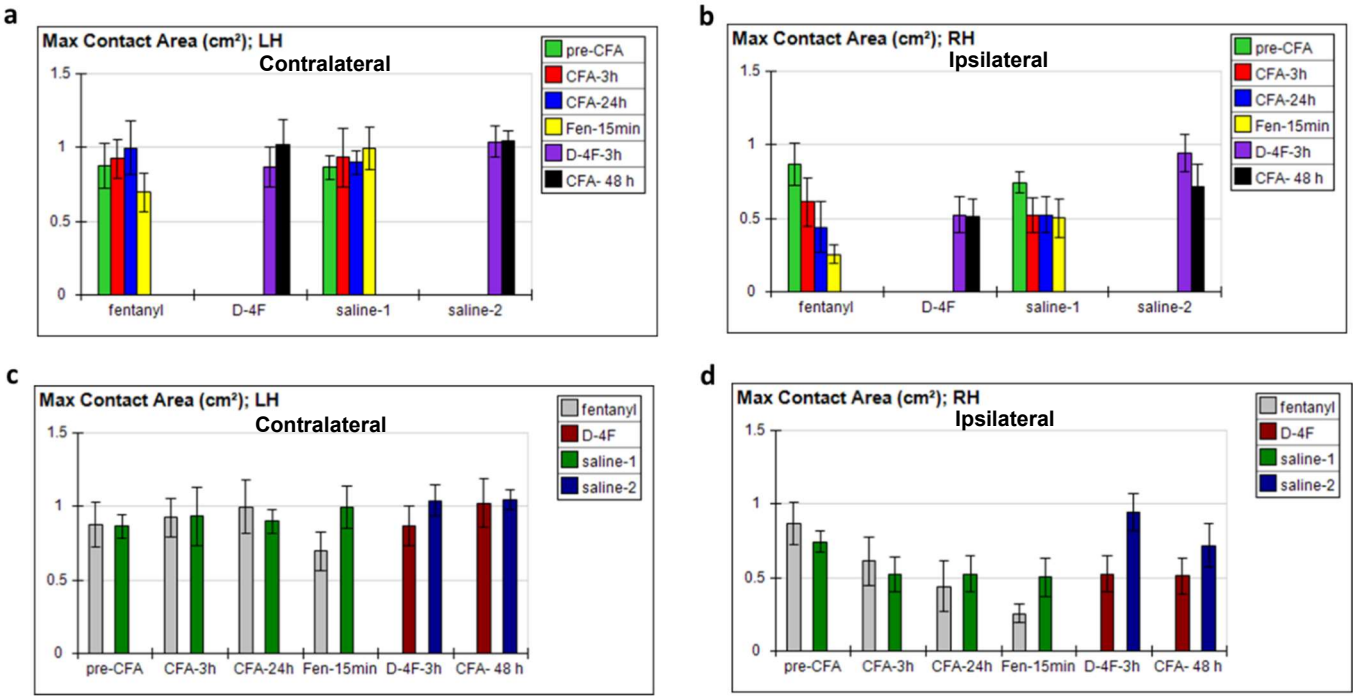

Figure 33 Effects of inflammation on maximum contact area of the rats' hind paw

Inflammation decreased maximum contact area in the ipsilateral paw (**b** and **d**) while it did not change in the contralateral paws (**a** and **c**). Fentanyl and D-4F treatments further decreased maximum contact area in both paws. Male Wistar rats were injected with 150 µl CFA in the ipsilateral hind paw after the baseline recording and were measured again 3 and 24 h after CFA injection. Then, 3 µg fentanyl in 100 µl saline was injected into the ipsilateral hind paw of the experimental group and the control group received vehicle. After 15 min, the gait was recorded. Forty-eight hours after CFA treatment, runs were again recorded and then 500 µg D-4F peptide in 100 µl saline was into the ipsilateral hind paw of the experimental group and the control group received vehicle. After 3 h, gait behavior was obtained for the last time. N = 6 per group

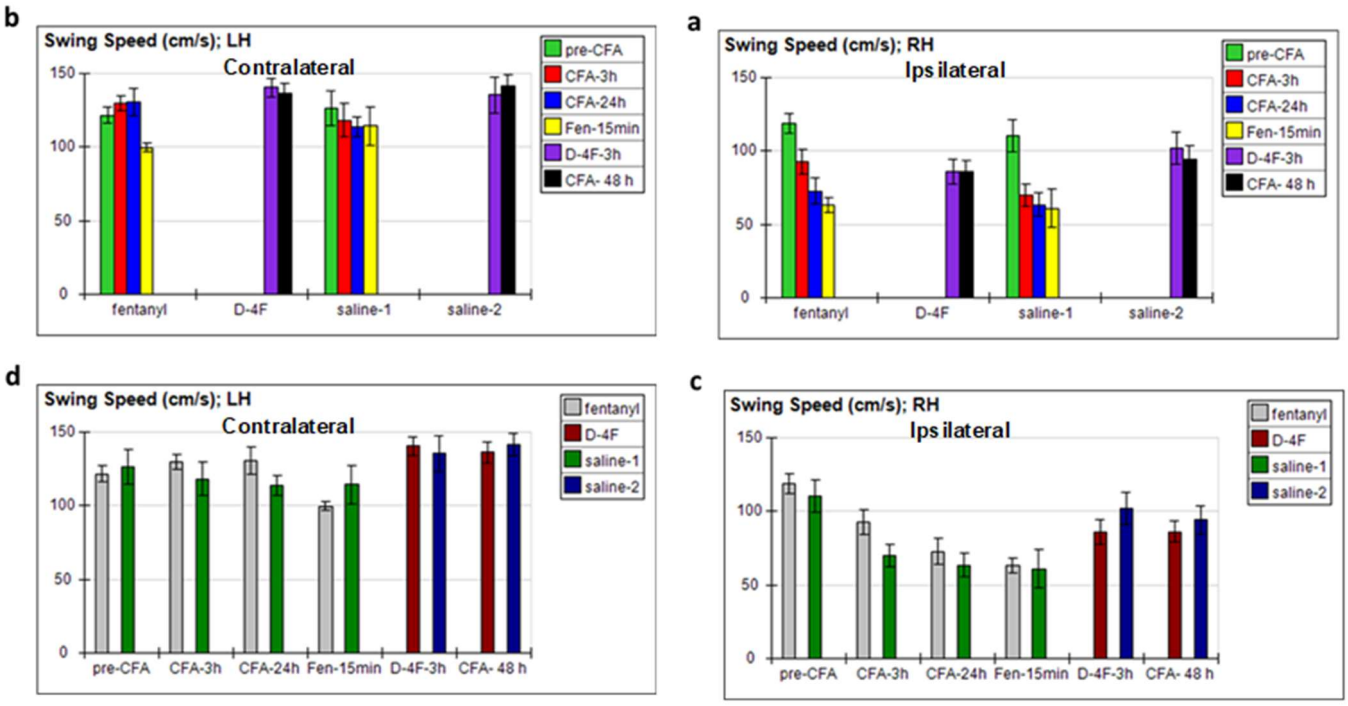

Figure 34 Effects of inflammation on swing speed of the rats' hind paw

Inflammation decreases swing speed in the ipsilateral paw (a and c) and increases it in the contralateral paws (b and d). Fentanyl decreases swing speed in the contralateral paw (b and d). Male Wistar rats were injected with 150 µl CFA in the ipsilateral hind paw after the baseline recording and were recorded again 3 and 24 h after CFA injection. Then 3 µg fentanyl in 100 µl saline was injected into the ipsilateral hind paw of the experimental group and the control group received vehicle. After 15 min, the animals' gaits were recorded. Forty-eight hours after CFA treatment the gait was recorded and then 500 µg D-4F peptide in 100 µl saline was into the ipsilateral hind paw of the experimental group and the control group received vehicle. After 3 h, gait behavior was recorded for the last time then animals were euthanized. N = 6 per group

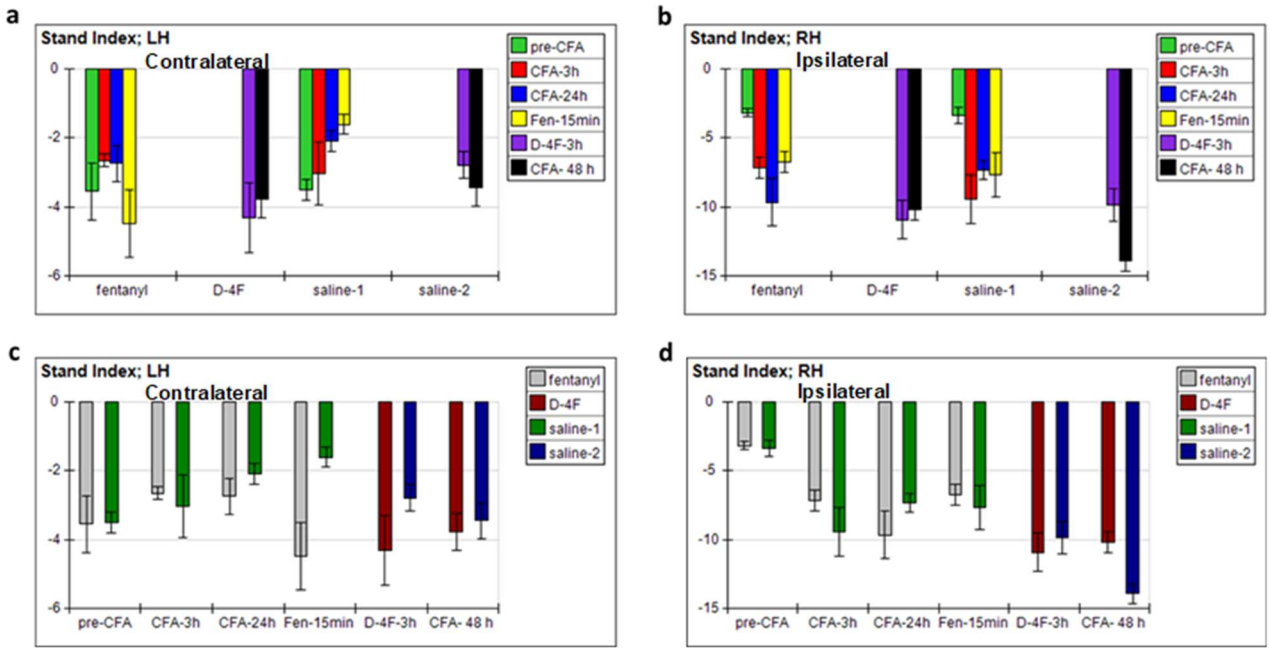

Figure 35 Effects of inflammation on stand index of the rats' hind paw

Inflammation decreased stand index in the ipsilateral paws (**b** and **d**) and increased it in the contralateral paws (**a** and **c**). Fentanyl treatment reversed these trends in both paws while D-4F treatment reversed the trend only in the contralateral paws. Male Wistar rats were injected with 150 µl CFA in the ipsilateral hind paw after the baseline recording and were recorded again 3 and 24 h after CFA injection. Then 3 µg fentanyl in 100 µl saline was injected into the ipsilateral hind paw of the experimental group and the control group received vehicle. After 15 min, the animals' gaits were recorded. Forty-eight hours after CFA treatment the gait was recorded and then 500 µg D-4F peptide in 100 µl saline was into the ipsilateral hind paw of the experimental group and the control group received vehicle. After 3 h, gait behavior was recorded for the last time then animals were euthanized. N = 6 per group

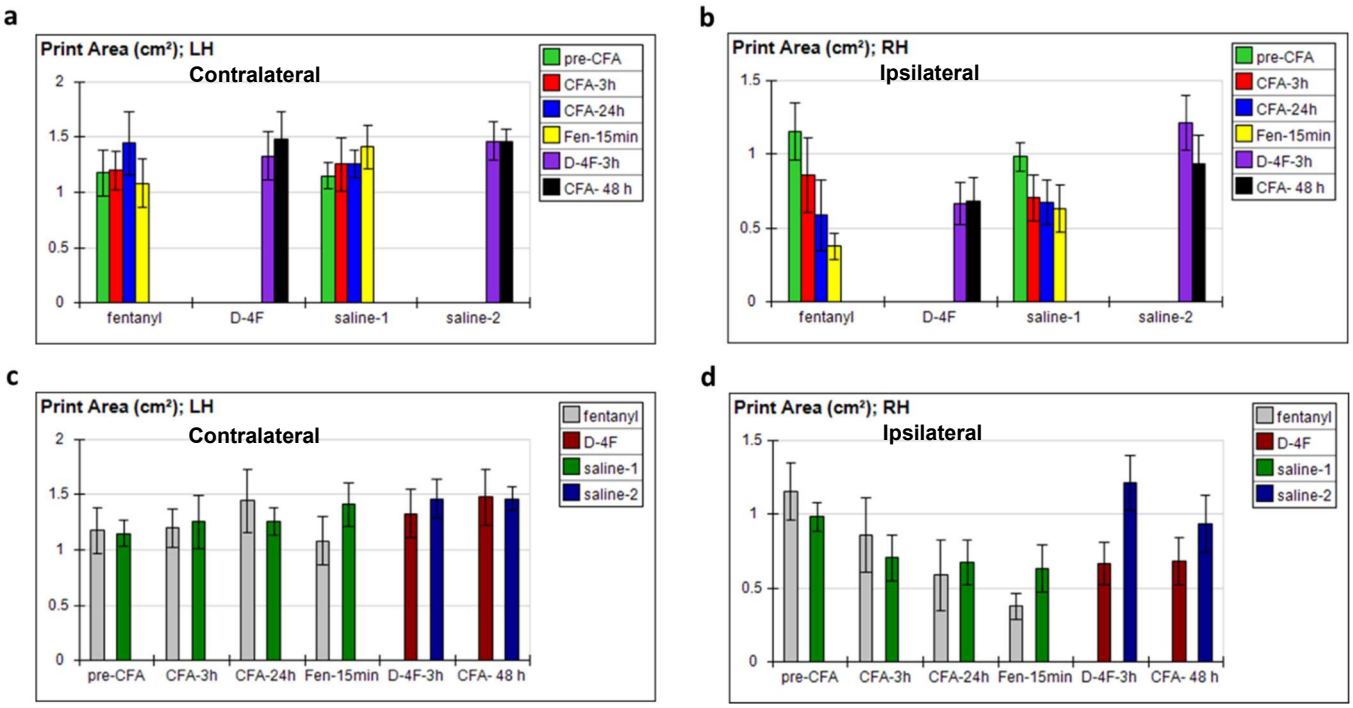

Figure 36 Effects of inflammation on print area of the rats' hind paw

Inflammation decreases print area in the ipsilateral paw (b and d) and slightly increases it in the contralateral paws (a and c). While fentanyl further decreases the print area in ipsilateral paw, D-4F treatments has no effect on ipsilateral paw. Male Wistar rats were injected with 150 µl CFA in the ipsilateral hind paw after the baseline recording and were recorded again 3 and 24 h after CFA injection. Then 3 µg fentanyl in 100 µl saline was injected into the ipsilateral hind paw of the experimental group and the control group received vehicle. After 15 min, the animals' gaits were recorded. Forty-eight hours after CFA treatment the runs were recorded and then 500 µg D-4F peptide in 100 µl saline was into the ipsilateral hind paw of the experimental group and the control group received vehicle. After 3 h, gait behavior was recorded for the last time then animals were euthanized. N = 6 per group

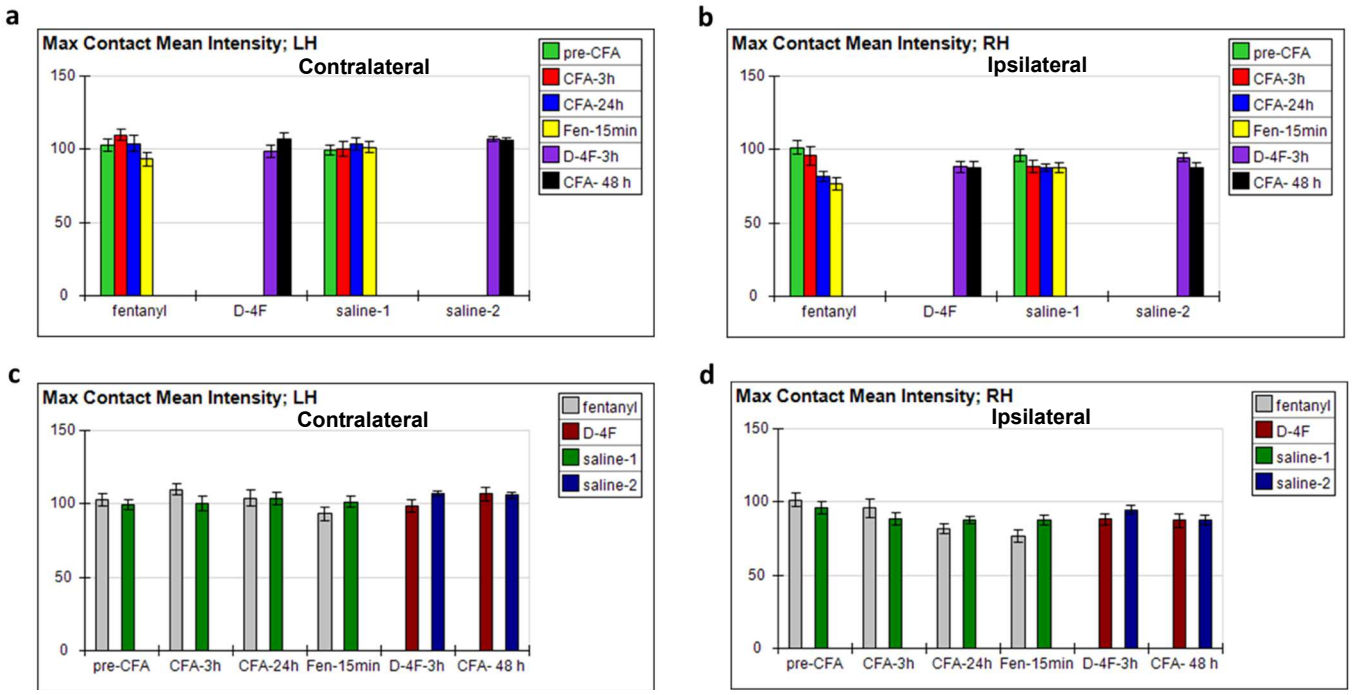

Figure 37 Effects of inflammation on max contact mean intensity of the rats' hind paw

Inflammation decreases max contact mean intensity in the ipsilateral paw (**b** and **d**) but not in the contralateral paws (**a** and **c**). While fentanyl decreases the max contact mean intensity in both paws, D-4F treatments has no effect on both paws. Male Wistar rats were injected with 150 µl CFA in the ipsilateral hind paw after the baseline recording and were recorded again 3 and 24 h after CFA injection. Then 3 µg fentanyl in 100 µl saline was injected into the ipsilateral hind paw of the experimental group and the control group received vehicle. After 15 min, the animals' gaits were recorded. Forty-eight hours after CFA treatment, runs were recorded and then 500 µg D-4F peptide in 100 µl saline was into the ipsilateral hind paw of the experimental group and the control group received vehicle. After 3 h, gait behavior was recorded for the last time then animals were euthanized. N = 6 per group

4. Discussion

Lipids are the essential building blocks of the bio-membrane and energy sources as well as important messengers in the organisms. In order to convey the messages within the system they should be structurally recognizable by the receptors (Bochkov, Gesslbauer, Mauerhofer, Philippova, Erne & Oskolkova, 2017). Thus, structural modifications such as oxidation is part of the process of transform structural lipids into messengers. Among these oxidized lipid messengers, OxPLs are gathering overwhelming attention and over 100 research articles per year were published in the last decade on the topic “oxidized phospholipids”.

The commercially obtained OxPAPC contains PAPC, POVPC, PGPC and PEIPC. POVPC and PGPC both stimulate TRPA1 and most likely elicit hyperalgesia (Bretscher et al., 2015). Selected OxPAPC components are so reactive with other molecules *in vivo* and thus are not stable while other like PGPC have a low reactivity. OxPAPC components such as POVPC covalently bind proteins and thus represent transient pathophysiological mediators. *In vitro,* non-oxidized PAPC is highly reactive on ambient air but in contrast, OxPAPC composition is stable of in ambient air for up to 5 h. In vivo, POVPC and PGPC were detected after immediate tissue retrieval and analysis by MALDI-TOF while other OxPAPC metabolites such as LPC were found regularly 15 min after OxPAPC injection (Oehler et al., 2017a).

When OxPAPC is injected intraplantarly, it induces long-lasting hypersensitivity behavior in rats and mice suggesting that not only it has a fast action as a stimulant of pain behavior but also may act as a key component in a cascade of proalgesic mediators leading to long-lasting inflammatory pain and sensitization. It was observed that acute OxPAPC-mediated activation of TRP channels was sufficient to release CGRP, thus, indicating that OxPAPC triggers elements of the molecular cascade leading to inflammatory pain. Antagonizing OxPAPC function was an efficient way to reduce immediate actions of OxPAPC stimuli such as calcium responses *in vitro* but also long-lasting hypersensitivity *in vivo* (Oehler et al., 2017a).

In vitro and *in vivo* evidences supports that TRPA1 is a major molecular target of OxPLs, although in higher doses OxPAPC modestly activates TRPV1. *In vitro* OxPAPC and components of OxPAPC such as PGPC and POVPC stimulate TRPA1-mediated ion influx in HEK_{TRPA1}. Also, the TRPA1 blocker HC-030031 inhibits acute OxPAPC-mediated calcium fluxes in DRG neurons. *In vitro*, OxPAPC-mediated CGRP release is significantly reduced in tissue from TRPA1 KO. Also, OxPAPC action *in vivo* is antagonized by the TRPA1 blocker HC-030031 and, is attenuated in TRPA1 KO (Oehler et al., 2017a; Martin et al., 2018).

Although some quantitative differences between species in their responses to OxPLs cannot be excluded, it seems that TRPA1 activation by OxPLs is species-independent. For instance, OxPAPC,

PGPC and POVPC activate recombinant human TRPA1, OxPAPC induces calcium influx in rat and mouse DRG neurons and OxPAPC-induced pain behavior was observed in the mouse and rat and was also observed in TRPV1 KO mice (Oehler et al., 2017a).

Pharmacological TRPA1 and TRPV1 blockade inhibits OxPAPC-induced mechanical hypersensitivity, while thermal hypersensitivity is only affected by TRPV1 in rats. TRPA1 and TRPV1 antagonists, TRPA1 KO, TRPV1 KO and TRPA1/TRPV1 double KO mice show reduced OxPAPC-triggered CGRP release, so it seems that both receptors contribute to OxPAPC-induced CGRP release. These results are in line with the previous research that shows TRPA1 is one of the main but not the only receptor of OxPLs on the nociceptors (Liu et al., 2016). TRPA1 in general plays an essential role in inflammatory mechanical sensitization and mechanical nocifensive reflexive behaviors (Lennertz, Kossyreva, Smith & Stucky, 2012; Zappia, O'Hara, Moehring, Kwan & Stucky, 2017).

In the cellular models, however, TRPA1 is the main targets of OxPAPC. It should be noted that the activity of TRPV1 depends on its phosphorylation status, which is raised by inflammatory mediators such as PGE2 and bradykinin, and also by TRPA1 activation itself, which stimulates protein kinase A-mediated phosphorylation (Li et al., 2014). TRPV1 activation might be also facilitated by intracellular phosphorylation induced by other OxPAPC-binding receptors (CD36, PAF receptor, toll like receptor 4, peroxisome proliferator-activated receptors, prostaglandin E2 receptor) on TRPV1 expressing neurons (Fruhwirth et al., 2014). Although OxPLs bind to prostaglandin E2 and prostaglandin D2 receptors, it has been shown that neither prostaglandin E2 nor prostaglandin D2 receptors do not play a sensitizing role in OxPAPC-induced TRPA1 activation in DRG neurons and HEK293 cells expressing TRPA1 (Liu *et al.*, 2016). It needs to be considered that *in vivo* inflammatory mediators are abundant in the CFA-injected paw. OxPAPC can induce Toll-like receptor 4 activation possibly in CCR2-expressing monocytes or macrophages, which then mediate indirect, sensitizing actions on TRPV1 function (Chen et al., 2009). In summary and based on genetic and pharmacological evidences *in vivo,* I suggest that TRPA1 is a major player in OxPLs-induced hypersensitivity.

E06 IgM mAb is a monoclonal antibody identical to T15, a natural IgA form B-1 cell origin, which protects mice against *S. pneumoniae* infections (Masmoudi, Mota-Santos, Huetz, Coutinho & Cazenave, 1990; Shaw et al., 2000). E06 mAb binds specifically to the oxidized head group of phospholipids such as OxPAPC (Friedman, Horkko, Steinberg, Witztum & Dennis, 2002; Thimmulappa, Gang, Kim, Sussan, Witztum & Biswal, 2012). E06 mAb has widely been used to detect OxPLs by immunohistochemistry or binding studies in several diseases e.g. acid-induced lung injury (Imai et al., 2008), arteriosclerosis (Ravandi et al., 2014; Shaw et al., 2000), bacterial peritonitis (Matt et al., 2013), multiple sclerosis (Haider et al., 2011) or inflammatory nephritis (Buga

et al., 2008) and age-related macular degeneration (Handa et al., 2015). Furthermore, E06 mAb as a blocker of OxPLs helped *in vitro* to elucidate mechanisms of OxPLs. For example, E06 mAb neutralizes pro-inflammatory effects of OxPLs on macrophages by blocking their attachment to scavenger receptors and TLRs (Imai et al., 2008).

In vivo, E06 mAb possess anti-inflammatory, anti-atherogenic and pro-resolving properties. Several *in vivo* functional studies have been conducted in rodents using systemic and local application routes. Systemic passive immunization with E06 mAb protects against atherosclerotic plaque development (Faria-Neto et al., 2006) presumably by facilitating apoptotic cell clearance (Shaw et al., 2000). Moreover, the development of inflammatory arthritis is abrogated by systemic administration of T15, the E06 mAb equivalent, via interaction of the antibody with the complement system, as part of the immune response (Chen et al., 2009). Local treatments, reducing costs and limiting off target effects, are additional therapeutic options. For example, local intranasal E06 mAb increases the uptake of OxPLs by macrophages in mice exposed to cigarette smoke (Chen et al., 2009). In the current study, I extended this potential by providing extra evidence for the usefulness of E06 mAb in the treatment of inflammatory pain.

I investigated antinociceptive properties of E06 mAb and showed that E06 mAb can block or reverse mechanical hypersensitivity in CFA-induced inflammation in rats with no effects on inflammatory thermal hypersensitivity. Also, E06 mAb co-incubation with OxPAPC prevents OxPAPC-induced thermal and mechanical hypersensitivity *in vivo*. After knowing that E06 mAb has a preventive effect on OxPLs pro-nociceptive activities upstream of TRPA1 and TRPV1 activation, I evaluated the significance of OxPLs in pain pathway downstream of TRPA1 and TRPV1 activation. Also, I separately investigated acute nociception *in vivo* on the one hand and mechanical and thermal hypersensitivity on the other hand, simply because they are relying on different mechanisms. Also, mechanical and thermal nociception rely on different receptors on nociceptors. Mechanical nociception is mediated by Piezo1, Piezo2, ATP-gated purinergic ion-channel P2X3 and TRPA1. While, thermal pain is mainly transduced by TRPV1 and TRPV2 (Gangadharan & Kuner, 2013). I induced hypersensitivity and neurogenic inflammation by intraplantar injection of TRPA1 and TRPV1 agonists. Interestingly, mechanical hypersensitivity induced by 4-HNE, AITC and capsaicin was blocked by E06 mAb co-injection, while E06 mAb had no effects on H_2O_2-induced mechanical hypersensitivity. Mechanical hypersensitivity reached its peak 1 h after capsaicin injection and 3 h after AITC, 4-HNE and H_2O_2 injections. In parallel, OxPLs in irritant-treated rat paws were significantly higher than saline-treated rat paws at above mentioned time points. Lastly, E06 mAb had no effects on thermal hypersensitivity induced by the said irritants. All of the irritants elicited reflexive nociceptive behavior to thermal and mechanical stimuli, nocifensive and affective motivational behavior. These findings are in line with the literature and further extend previous reports. Besides the known tactile allodynia (von Frey) and nocifensive response (Trevisani et al.,

2007a), 4-HNE elicits also thermal hypersensitivity and a few affective motivational nociceptive responses. Local application of H_2O_2 causes mechanical and thermal hypersensitivity as well as nocifensive behavior (Keeble et al., 2009), visceral bladder pain (Nicholas, Yuan, Brookes, Spencer & Zagorodnyuk, 2017), edema, cold allodynia, and ongoing nociception (Trevisan et al., 2013b). In addition, H_2O_2 evokes pronounced affective motivational nociceptive responses. AITC as well as capsaicin trigger mechanical and thermal hypersensitivity (Bautista et al., 2006; Endres-Becker et al., 2007). Both also initiate spontaneous nocifensive and affective motivational nociceptive. Especially capsaicin elicits pronounced affective motivational behavior. In summary, I propose that H_2O_2 elicit the formation of proalgesic mediators activating heat sensors except of OxPLs that are not captured by E06 mAb.

Based on the *in vitro* experiments, I suggested that 4-HNE binds to E06 mAb, because preincubation of E06 mAb with 4-HNE prevented calcium influx in HEK_{TRPA1}cells as well as in DRG neurons. It has been shown that E06 mAb does not bind to 4-HNE coupled to LDL (Palinski et al., 1996). By extending these observations, I provided evidence that neither 4-HNE itself nor 4-HNE-BSA bind to E06 mAb. In a similar fashion, direct interactions of AITC or capsaicin with E06 mAb are very unlikely because of the lack of homologies between theses irritants and OxPLs.

Considering the high affinity and specificity of E06 mAb to phosphorylcholine (PC) head group of OxPLs I suggested an indirect mechanism in which irritants elicit OxPLs formation and OxPLs in paw tissue. It should also be noted that OxPLs are very pro-inflammatory and likely promote a local cycle of inflammation that in turn generates more OxPLs.

Mechanical hypersensitivity induced by H_2O_2 was non-respondent to E06 mAb blockade. It should be noted that unlike the other irritants used in this study activating either TRPA1 or TRPV1 in the given doses, H_2O_2 not only is a highly reactive radical that activates TRPA1 and readily sensitize TRPV1 and triggers different mechanisms underlying inflammatory pain (Chuang & Lin, 2009; Keeble et al., 2009) but also TRPM2 and TRPC5 (Andersson, Gentry, Moss & Bevan, 2008; DelloStritto et al., 2016; Naylor et al., 2011). The peroxide triggers different mechanisms underlying inflammatory pain by direct receptor interaction or by increased expression of pro-inflammatory cytokines and chemokines (Chung, Asgar, Lee, Shim, Dumler & Ro, 2015; Keeble et al., 2009). Indeed, also the peroxide sensor TRPM2 is expressed on DRGs (Sumoza-Toledo and Penner, 2011). Taken together the data indicate that direct activation of TRP channels by H_2O_2 is not the unique pain-mediating pathway. If E06 mAb does not directly interact with H_2O_2, and therefore, neutralizes the substance, the blocking capability of the antibody is reduced.

ApoA-I mimetic peptides are known to have anti-inflammatory and anti-atherosclerotic activity *in vivo* (Van Lenten et al., 2008; Nandekar et al., 2011; Getz et al., 2010). In this study, I tested whether local administration of D-4F has an antinociceptive effect in animal models of acute inflammation

and irritant induced hypersensitivity. In all tested conditions, D-4F treatment blocked the development of mechanical hypersensitivity with some effects on thermal hypersensitivity. Mechanistically, I suggest that the antinociceptive property of D-4F is due to a scavenger-like inhibition of OxPLs function, thus antagonizing the pro-inflammatory and pro-nociceptive properties of OxPLs metabolites.

E06 mAb prevented inflammatory hypersensitivity evoked by CFA and OxPAPC and also prolonged mechanical hypersensitivity induced by 4-HNE, capsaicin and AITC. In our study, thermal hypersensitivity was not affected by E06 mAb treatment that is line with the data showing OxPLs only in high doses and modestly activate TRPV1 which is essential for thermal hypersensitivity.

Although most research into the role of TRPA1/V1 channels in pain has focused on functions of these channels on nociceptors, there are accumulation data suggesting an important role of these channels in non-neuronal cells (reviewed by (Fernandes, Fernandes & Keeble, 2012) TRPA1/V1 are functionally expressed on keratinocytes (Inoue, Koizumi, Fuziwara, Denda, Inoue & Denda, 2002). Activation of TRPA1 on keratinocytes and fibroblasts leads to secretion of the eicosanoids, such as prostaglandin E2 and leukotriene B4 (LTB4) and evokes a long-lasting local erythema (Jain, Bronneke, Kolbe, Stab, Wenck & Neufang, 2011). TRPA1 is also expressed by melanocytes affecting the expression of pro-inflammatory cytokines, including IL-1α, IL-1β (Atoyan, Shander & Botchkareva, 2009; Nilius, Appendino & Owsianik, 2012). This suggest that activation of TRPA1 by OxPLs on non-neuronal cells could contribute to the vicious circle in inflammation and possibly hypersensitivity.

Different thermo-sensitive ion channels are activated in different temperature ranges and thus the knowledge of the exact temperature of the thermal withdrawal threshold would be interesting to narrow down responsible channels (Vay et al., 2012; Vandewauw et al., 2018). The plantar method (also known as Hargreaves method) uses radiant heat as the thermal stimulus (that is non-quantifiable) and utilizes the latency of withdrawal as an indirect indicator of thermal threshold. It provides the measurement of ipsilateral (treated hind paw) and contralateral (non-treated hind paw) heat thresholds when each animal serves as its own internal control, unlike other methods such as the hot plate tests where all four paws and the tail are in contact with the heated metal surface. But the disadvantage of this method is that it will not provide the actual temperature of withdrawal. The actual temperature of the animal's paw depends on many factors such as temperature of the glass floor, intensity of the radiant heat, the area of the paw illuminated and radiation density.

Although determining the actual temperature of the paws in our experiments would not be possible, it can be postulated on basis of the published data. Ken Hargreaves in his original report (Hargreaves, Dubner, Brown, Flores, & Joris, 1988) has used a contact thermocouple to directly measure and report paw's temperature. Based on Hargreaves observations, hind paw temperature

of comparable rats (male 250-300 g) was 27.9 ± 0.2 ˚C, while the temperature of carrageenan-injected paws (inflamed) were slightly higher (30.5 ± 0.2 ˚C). Withdrawal latency of the inflamed paws was 3.5 ± 0.6 s in comparison to 10.9 ± 0.6 of saline injected paws. This corresponded to 38.5 ± 0.7 ˚C and 45.2 ± 0.2 ˚C for inflamed and non-inflamed paws, respectively. Considering the similarity between our control data and the published data and by comparing the withdrawal latencies, we can conclude that the baseline paw temperature in our experiments was close to ~ 38 C˚ and thermal threshold of the control paws is estimated to be ~ 45 ˚C.

There are several individual TRP channels that are recognized as thermo-TRPs. They are expressed in primary somatosensory neurons and are activated at specific temperatures in the range from noxious heat to painful cold of which TRPV1 and TRPV2 are considered to be involved in sensation of noxious heat (Vay et al., 2012). Considering that activations temperature is ≥42°C for TRPV1 and ≥52°C for TRPV2, we can assume that in our experiments TRPV1 was playing a more important role since the paw temperature has never exceeded ~ 45 C˚ that is far below TRPV2 activation threshold. However, the exact complex mechanisms of thermal nociception is yet to be illuminated. For instance, recently it was shown that a trio of TRP channels (TRPA1, TRPV1 and TRPM3) mediate acute heat nociception in concert (Vandewauw et al., 2018).

Using animal models in preclinical and basic pain research is inevitable and conventional techniques to supposedly measure hypersensitivity and allodynia were in usage for the last 60 years. These conventional methods mostly rely on measuring reflexive behaviors in response to mechanical or thermal stimuli. However, quantifying spontaneous ongoing pain in an objective way was always a challenge. Also, such reflexive behaviors are rather indicators of animal's "hypersensitivity" to external stimuli and attributing them to pain, hypersensitivity or allodynia is rather an overgeneralization of human behavior. Measuring persistent (ongoing) pain in animal models is clinically relevant and has higher translational value. It’s different from hypersensitivity on the basis of the mechanisms involved. So far, spontaneous nocifensive reflexes such as flinching, guarding, shaking or licking of the hind paw were used to assess ongoing pain. Although, this gives a way to measure ongoing pain, it’s limited to models involving the hind paw and is prone to the experimenters’ bias and subjectivity. To this end, inventing sensitive and specific imaging methods for quantifying spontaneous pain could contribute to a better understanding of this phenomenon (Tappe-Theodor & Kuner, 2014).

Over past decade, several groups have tried to use dynamic wear bearing in free moving animals as an index of functional and translatable read out in pain assessment. It is postulated that such non-evoked and voluntary behavior has more translational value and more relevance to human pain conditions in comparison to evoked methods such as paw pressure threshold or paw withdrawal latency. Although, there are many examples of successful application of CatWalk in quantitative

pain measurement, utilizing such innovative methods has not be hassle free (Mogil et al.,2010; Huehnchen et al.,2013). For instance, although mechanical allodynia and CatWalk parameters show a high correlation in acute carrageenan-induced knee monoarthritis model (Gabriel et al.,2007), no correlation between development of mechanical allodynia and Catwalk parameters have been found in chronic carrageenan-induced knee monoarthritis (Gabriel *et al.*,2009). Also, many factors demonstrate adequate face validity in determining the establishment of the pain model but may fail to provide enough predictive validity once analgesic treatments are applied (Mogil et al.,2010; Huehnchen et al.,2013). For instance, in a study to evaluate chemotherapy-induced polyneuropathy in mice, CatWalk was used in comparison to traditional von Frey test (Huehnchen et al.,2013). While gabapentin reversed neuropathy-induced mechanical hypersensitivity and the duty cycle in CatWalk, it failed to reverse neuropathy-induced print area reduction.

Max contact mean intensity and print area are presumably among the most critical factors to evaluate hypersensitivity to pressure. As expected, after CFA injection, they start to decrease as an indication of mechanical hypersensitivity. In other words, because the paw becomes inflammaed and painfull, the animal avoids bearing weight on them and thus pressing them to the floor while gaiting. The rational hypothesis would be that fentanyl injection would decrease the pain and hypersensitivity and we will observe increasing max contact mean intensity and print area after the opioid adminstration. Contrary to the anticipation, max contact mean intensity and print area continue to shrink after fentanyl injection. CatWalk relies on video recording of paw prints on a glass floor. Thus, any factor that deforms the paw shape will affect the data. One of the most important interferring factors in evaluation of CFA model by CatWalk is the paw edema due to inflammation. In all of the studies with sucessful usage of CatWalk, either neuropathic or monoartheritic inflammatory painmodel have been utilized because could inflammatory paw edema interferes with many recorded factors. For intance, although Pitzer *et al*. (2016) showed that stand and swing durations will be effected by CFA inflammation in mice paw. However, they did not prove that these changes can be rescued by an anagesic treatment. Administration of opioids (like fentanyl) will aleviate inflammatory pain, but it has no effects on the inflammatory paw edema. So, this could be one of the main reasons why fentanyl failed to revered CFA-induced changes. Also, it should be noted that injection *per se* (100-150 µl) will change the volume of the paw in short term and thus will change the recorded factors accordingly. As a solution to this problem int the future, I would suggest smaller volumes of injection (20 µl max) and longer interval between the injection and recording trials.

In line with my observations, it has been shown that some CatWalk parameters change after SNI but not CCI surgery in mice. However, these changes are not reversable by different analgesics such as morphine and EMLA, while mechanical hpersensitivity was perfectly revesrsed by these

treatments (Mogil et al.,2010). In summary, my findings does not support CatWalk utilization as a robust and objective assessment method in CFA inflammatory pain.

5. Conclusion

My results show that OxPLs accumulate in the inflamed tissue as well as down-stream of TRPA1 and TRPV1 activation. Not only injection of OxPAPC induces hypersensitivity, but also antagonism of the action of OxPLs blocks mostly mechanical and to some extend thermal hypersensitivity in inflammatory models in rodents. In addition, pharmacologic blockade or genetic knock out of TRPA1 sufficiently attenuate pro-nociceptive effects of OxPAPC intraplantar injections, suggesting that TRPA1 is a major molecular target of OxPLs in mediating pronociceptive effects. Considering the critical role of OxPLs and OSEs in development of inflammatory conditions, understanding the underlying molecular mechanisms of OSE-induced inflammation and pain as well as determining the potency of natural anti-OSE compounds such as E06 mAb/T15 type mAb in antagonizing inflammatory conditions could contribute to the development of novel therapeutic interventions, like analgesics.

My results are suggesting two options to antagonize *in vivo* pronociceptive properties of OxPLs. To antagonize OxPLs activity, I introduced local application of a monoclonal antibody (E06 mAb) and the ApoA-I mimetic peptide D-4F. Interestingly, E06 mAb and D-4F peptide inhibit mechanical hypersensitivity in Wistar rats induced by OxPAPC, CFA, 4-HNE, capsaicin and AITC, most likely by scavenging OxPLs. In parallel, while E06 mAb does not have any effects on thermal hypersensitivity induced by aforementioned agents and hydrogen peroxide, D-4F peptide blocks thermal hypersensitivity induced by 4-HNE and capsaicin but has no effect on the thermal hypersensitivity induced by other mentioned irritants. In addition, mechanical hypersensitivity induced by hydrogen peroxide is blocked by D-4F but not E06 mAb. Further studies are required in order to understand the role of OxPLs in other types of pain e.g. neuropathic pain, chemotherapy-induced pain or bone cancer pain. Also, the potential of E06 mAb and D-4F peptide as candidate therapeutic drugs in inflammatory and other pain types should be investigated.

6. Appendix

4.1 **Values for κ, based on response pattern adopted from (Chaplan, Bach, Pogrel, Chung & Yaksh, 1994; Dixon, 1980)**

Pattern	Value for *k*	Pattern	Value for *k*	Pattern	Value for *k*	Pattern	Value for
OX	−0.5	OOOXOOOO	−0.547	XO	0.5	XXXOXXXX	0.547
OOX	−0.388	OOOOXOOOO	−0.547	XXO	0.388	XXXXOXXXX	0.547
OOOX	−0.378	OXOOOX	−1.25	XXXO	0.378	XOXXXO	1.25
OOOOX	−0.377	OOXOOOX	−1.247	XXXXO	0.377	XXOXXXO	1.247
OXO	0.842	OOOXOOOX	−1.246	XOX	−0.842	XXXOXXXO	1.246
OOXO	0.89	OOOOXOOOX	−1.246	XXOX	−0.89	XXXXOXXXO	1.246
OOOXO	0.894	OXOOXO	0.372	XXXOX	−0.894	XOXXOX	−0.372
OOOOXO	0.894	OOXOOXO	0.38	XXXXOX	−0.894	XXOXXOX	−0.38
OXX	−0.178	OOOXOOXO	0.381	XOO	0.178	XXXOXXOX	−0.381
OOXX	0	OOOOXOOXO	0.381	XXOO	0	XXXXOXXOX	−0.381
OOOXX	0.026	OXOOXX	−0.169	XXXOO	−0.026	XOXXOO	0.169
OOOOXX	0.028	OOXOOXX	−0.144	XXXXOO	−0.028	XXOXXOO	0.144
OXOO	0.299	OOOXOOXX	−0.142	XOXX	−0.299	XXXOXXOO	0.142
OOXOO	0.314	OOOOXOOXX	−0.142	XXOXX	−0.314	XXXXOXXOO	0.142
OOOXOO	0.315	OXOXOO	0.022	XXXOXX	−0.315	XOXOXX	−0.022
OOOOXOO	0.315	OOXOXOO	0.039	XXXXOXX	−0.315	XXOXOXX	−0.039
OXOX	−0.5	OOOXOXOO	0.04	XOXO	0.5	XXXOXOXX	−0.04
OOXOX	−0.439	OOOOXOXOO	0.04	XXOXO	0.439	XXXXOXOXX	−0.04
OOOXOX	−0.432	OXOXOX	−0.5	XXXOXO	0.432	XOXOXO	0.5
OOOOXOX	−0.432	OOXOXOX	−0.458	XXXXOXO	0.432	XXOXOXO	0.458
OXXO	1	OOOXOXOX	−0.453	XOOX	−1	XXXOXOXO	0.453
OOXXO	1.122	OOOOXOXOX	−0.453	XXOOX	−1.122	XXXXOXOXO	0.453
OOOXXO	1.139	OXOXXO	1.169	XXXOOX	−1.139	XOXOOX	−1.169
OOOOXXO	1.14	OOXOXXO	1.237	XXXXOOX	−1.14	XXOXOOX	−1.237
OXXX	0.194	OOOXOXXO	1.247	XOOO	−0.194	XXXOXOOX	−1.247
OOXXX	0.449	OOOOXOXXO	1.248	XXOOO	−0.449	XXXXOXOOX	−1.248
OOOXXX	0.5	OXOXXX	0.611	XXXOOO	−0.5	XOXOOO	−0.611
OOOOXXX	0.506	OOXOXXX	0.732	XXXXOOO	−0.506	XXOXOOO	−0.732
OXOOO	−0.157	OOOXOXXX	0.756	XOXXX	0.157	XXXOXOOO	−0.756
OOXOOO	−0.154	OOOOXOXXX	0.758	XXOXXX	0.154	XXXXOXOOO	−0.758
OOOXOOO	−0.154	OXXOOO	−0.296	XXXOXXX	0.154	XOOXXX	0.296
OOOOXOOO	−0.154	OOXXOOO	−0.266	XXXXOXXX	0.154	XXOOXXX	0.266
OXOOX	−0.878	OOOXXOOO	−0.263	XOXXO	0.878	XXXOOXXX	0.263
OOXOOX	−0.861	OOOOXXOOO	−0.263	XXOXXO	0.861	XXXXOOXXX	0.263
OOOXOOX	−0.86	OXXOOX	−0.831	XXXOXXO	0.86	XOOXXO	0.831
OOOOXOOX	−0.86	OOXXOOX	−0.763	XXXXOXXO	0.86	XXOOXXO	0.763
OXOXO	0.701	OOOXXOOX	−0.753	XOXOX	−0.701	XXXOOXXO	0.753
OOXOXO	0.737	OOOOXXOOX	−0.752	XXOXOX	−0.737	XXXXOOXXO	0.752
OOOXOXO	0.741	OXXOXO	0.831	XXXOXOX	−0.741	XOOXOX	−0.831
OOOOXOXO	0.741	OOXXOXO	0.935	XXXXOXOX	−0.741	XXOOXOX	−0.935
OXOXX	0.084	OOOXXOXO	0.952	XOXOO	−0.084	XXXOOXOX	−0.952
OOXOXX	0.169	OOOOXXOXO	0.954	XXOXOO	−0.169	XXXXOOXOX	−0.954
OOOXOXX	0.181	OXXOXX	0.296	XXXOXOO	−0.181	XOOXOO	−0.296
OOOOXOXX	0.182	OOXXOXX	0.463	XXXXOXOO	−0.182	XXOOXOO	−0.463
OXXOO	0.305	OOOXXOXX	0.5	XOOXX	−0.305	XXXOOXOO	−0.5
OOXXOO	0.372	OOOOXXOXX	0.504	XXOOXX	−0.372	XXXXOOXOO	−0.504
OOOXXOO	0.38	OXXXOO	0.5	XXXOOXX	−0.38	XOOOXX	−0.5
OOOOXXOO	0.381	OOXXXOO	0.648	XXXXOOXX	−0.381	XXOOOXX	−0.648
OXXOX	−0.305	OOOXXXOO	0.678	XOOXO	0.305	XXXOOOXX	−0.678
OOXXOX	−0.169	OOOOXXXOO	0.681	XXOOXO	0.169	XXXXOOOXX	−0.681
OOOXXOX	−0.144	OXXXOX	−0.043	XXXOOXO	0.144	XOOOXO	0.043
OOOOXXOX	−0.142	OOXXXOX	0.187	XXXXOOXO	0.142	XXOOOXO	−0.187
OXXXO	1.288	OOOXXXOX	0.244	XOOOX	−1.288	XXXOOOXO	−0.244
OOXXXO	1.5	OOOOXXXOX	0.252	XXOOOX	−1.5	XXXXOOOXO	−0.252
OOOXXXO	1.544	OXXXXO	1.603	XXXOOOX	−1.544	XOOOOX	−1.603
OOOOXXXO	1.549	OOXXXXO	1.917	XXXXOOOX	−1.549	XXOOOOX	−1.917
OXXXX	0.555	OOOXXXXO	2	XOOOO	−0.555	XXXOOOOX	−2
OOXXXX	0.897	OOOOXXXXO	2.014	XXOOOO	−0.897	XXXXOOOOX	−2.014
OOOXXXX	0.985	OXXXXX	0.893	XXXOOOO	−0.985	XOOOOO	−0.983
OOOOXXXX	1	OOXXXXX	1.329	XXXXOOOO	−1	XXOOOOO	−1.329
OXOOOO	−0.547	OOOXXXXX	1.465	XOXXXX	0.547	XXXOOOOO	−1.465
OOXOOOO	−0.547	OOOOXXXXX	1.496	XXOXXXX	0.547	XXXXOOOOO	−1.496

4.2 Summary and assignments of (phospho) lipids detected by positive ion MALDI-TOF mass spectrometry [a]. adapted from (Oehler et al., 2017a)

2 Integer m/z values are given.

The differentiation between triacylglycerols and hydroxylated triacylglycerols was made because CFA contains large amounts of castor oil, which contains considerable amounts of hydroxylated fatty acids. (*) Peaks at m/z 594.5 and 610.5 are derived from PAPC upon cleavage of the double bond next to the glycerol backbone. LPC, lysophosphatidylcholine; PC, phosphatidylcholine.

Lipid species	Peak Position (*m/z*)	Assignment of Molecular Mass
Oxidized PAPC (LPC)	496	LPC 16:0 (H^+)
	518	LPC 16:0 (Na^+)
	524	LPC 18:0 (H^+)
	546	LPC 18:0 (Na^+)
	551	Trimer of 2,5-Dihydroxybenzoic acid - $3H^+$ + $4Na^+$ (Gas phase)
Fragments of triacylglycerol	575	Fragment of triacylglycerol
	579	Fragment of triacylglycerol
	594	Aldehyde derived from PAPC (*); POVPC
	610	Carboxylic acid derived from PAPC (*); PGPC (H^+)
Fragments of triacylglycerol	601	Fragment of triacylglycerol
	616	Aldehyde derived from PAPC (*); POVPC
	620	Ceramide-1-phosphate d18:0/16:0 (H^+)
	632	Carboxylic acid derived from PAPC (*); PGPC (Na^+)
	648	Cerarmide 18:1/24:1 (H^+)
Fragments of triacylglycerol	689	Fragment derived from *m/z* 953.8
	715	Fragment derived from *m/z* 979.8

	725	Sphingomyelin 16:0 (Na^+)
PC species	734	PC 16:0/16:0 (H^+)
	756	PC 16:0/16:0 (Na^+)
	758	PC 16:0/18:2 (H^+)
	760	PC 16:0/18:1 (H^+)
	780	PC 16:0/18:2 (Na^+)
	782	PC 16:0/18:1 (Na^+) or PC 16:0/20:4 (H^+); unoxidized PAPC
	804	PC 16:0/20:4 (Na^+)
	806	PC 16:0/22:6 (H^+); PEIPC
	810	PC 18:0/20:4 (H^+); PECPC
	822	Triacylglycerol 48:1
PC species	828	PC 16:0/22:6 (Na^+); PEIPC
	832	PC 18:0/20:4 (Na^+); PECPC
Hydroxylated triacylglycerols	953	Triacylglycerol (1×18:2-OH, 2×18:1-OH) (Na^+)
	979	Triacylglycerol (2×18:0-OH, 1×18:0-$(OH)_2$) (Na^+)

List of tables

List of figures

7. Affidavit

I hereby confirm that my thesis entitled “Role of oxidized phospholipids in inflammatory pain (Rolle von oxidierten Phospholipiden bei entzündlichen Schmerzen)” is the result of my own work. I did not receive any help or support from commercial consultants. All sources and / or materials applied are listed and specified in the thesis.

Furthermore, I confirm that this thesis has not yet been submitted as part of another examination process neither in identical nor in similar form.

Place, Date Signature

Eidesstattliche Erklärung

Hiermit erkläre ich an Eides statt, die Dissertation „Role of oxidized phospholipids in inflammatory pain (Rolle von oxidierten Phospholipiden bei entzündlichen Schmerzen)“ eigenständig, d.h. insbesondere selbstständig und ohne Hilfe eines kommerziellen Promotionsberaters, angefertigt und keine anderen als die von mir angegebenen Quellen und Hilfsmittel verwendet zu haben.

Ich erkläre außerdem, dass die Dissertation weder in gleicher noch in ähnlicher Form bereits in einem anderen Prüfungsverfahren vorgelegen hat.

Ort, Datum Unterschrift

8. Acknowledgments

Dear Prof. Heike L. Rittner, I would like to express my sincere gratitude for giving me this opportunity and supervising my PhD project, Thank you for everything.

I would like to thank the members of my thesis committee: Dr. Robert Blum, Dr. Beatrice Oehler and Dr. Nurcan Üçeyler.

My special thanks to Anja, Katy, Egle and Jeremy for assisting me through my work.

I sincerely thank the excellent funding from IZKF that made this challenging research work possible. I would also like to thank Graduate School of Life Science Würzburg for the administrative assistance, travel fellowships and additional trainings support during the period of my PhD.

I am very thankful to my family and friends. First, I would like to thank my wife Pantea, for her patience and continuous support throughout my PhD. Without your love and support this work would have remained a dream.

10. References

Al-Shawaf E, Naylor J, Taylor H, Riches K, Milligan CJ, O'Regan D, et al. (2010). Short-term stimulation of calcium-permeable transient receptor potential canonical 5-containing channels by oxidized phospholipids. Arteriosclerosis, Thrombosis, and Vascular Biology 30(7): 1453-1459.

Ambrogini E, Que X, Wang S, Yamaguchi F, Weinstein RS, Tsimikas S, Manolagas SC, Witztum JL, Jilka RL. (2018) Oxidation-specific epitopes restrain bone formation. Nature Communications 9(1):2193.

Andersson DA, Gentry C, Moss S, Bevan S (2008). Transient receptor potential A1 is a sensory receptor for multiple products of oxidative stress. The Journal of neuroscience 28(10): 2485-2494.

Atoyan R, Shander D, Botchkareva NV (2009). Non-neuronal expression of transient receptor potential type A1 (TRPA1) in human skin. Journal of Investigative Dermatology 129.

Babes A, Sauer SK, Moparthi L, Kichko TI (2016). Photosensitization in Porphyrias and Photodynamic Therapy Involves TRPA1 and TRPV1. The Journal of Neuroscience 36(19): 5264-5278.

Bautista DM, Jordt SE, Nikai T, Tsuruda PR, Read AJ, Poblete J, et al. (2006). TRPA1 mediates the inflammatory actions of environmental irritants and proalgesic agents. Cell 124(6): 1269-1282.

Binder CJ (2010). Natural IgM antibodies against oxidation-specific epitopes. Journal of clinical immunology 30 Suppl 1: S56-60.

Binder CJ, Horkko S, Dewan A, Chang MK, Kieu EP, Goodyear CS, et al. (2003). Pneumococcal vaccination decreases atherosclerotic lesion formation: molecular mimicry between Streptococcus pneumoniae and oxidized LDL. Nature medicine 9(6): 736-743.

Binder CJ, Papac-Milicevic N, Witztum JL (2016). Innate sensing of oxidation-specific epitopes in health and disease. Nature reviews. Immunology 16(8): 485-497.

Bochkov V, Gesslbauer B, Mauerhofer C, Philippova M, Erne P, Oskolkova OV (2017). Pleiotropic effects of oxidized phospholipids. Free radical biology & medicine 111: 6-24.

Bochkov V, Schoenenberger AW, Oskolkova O, Toth U, Stockl J, Majdic O, et al. (2016). Novel immune assay for quantification of plasma protective capacity against oxidized phospholipids. Biomarkers in medicine 10(8): 797-810.

Bochkov VN, Oskolkova OV, Birukov KG, Levonen A-L, Binder CJ, Stöckl J (2009). Generation and Biological Activities of Oxidized Phospholipids. Antioxidants & Redox Signaling 12(8): 1009-1059.

Brederson J-D, Kym PR, Szallasi A (2013). Targeting TRP channels for pain relief. European Journal of Pharmacology 716(1–3): 61-76.

Bretscher P, Egger J, Shamshiev A, Trötzmüller M, Köfeler H, Carreira EM, et al. (2015). Phospholipid oxidation generates potent anti-inflammatory lipid mediators that mimic structurally related pro-resolving eicosanoids by activating Nrf2. EMBO Molecular Medicine 7(5): 593-607.

Buga GM, Frank JS, Mottino GA, Hakhamian A, Narasimha A, Watson AD, et al. (2008). D-4F reduces EO6 immunoreactivity, SREBP-1c mRNA levels, and renal inflammation in LDL receptor-null mice fed a Western diet. Journal of Lipid Research 49(1): 192-205.

Chaplan SR, Bach FW, Pogrel JW, Chung JM, Yaksh TL (1994). Quantitative assessment of tactile allodynia in the rat paw. Journal of neuroscience methods 53(1): 55-63.

Charles-Schoeman C, Banquerigo ML, Hama S, Navab M, Park GS, Van Lenten BJ, et al. (2008). Treatment with an apolipoprotein A-1 mimetic peptide in combination with pravastatin inhibits collagen-induced arthritis. Clinical immunology (Orlando, Fla.) 127(2): 234-244.

Chattopadhyay A, Navab M, Hough G, Grijalva V, Mukherjee P, Fogelman HR, et al. (2016). Tg6F ameliorates the increase in oxidized phospholipids in the jejunum of mice fed unsaturated LysoPC or WD. Journal of Lipid Research 57(5): 832-847.

Chen Y, Khanna S, Goodyear CS, Park YB, Raz E, Thiel S, et al. (2009). Regulation of dendritic cells and macrophages by an anti-apoptotic cell natural antibody that suppresses TLR responses and inhibits inflammatory arthritis. Journal of immunology 183(2): 1346-1359.

Chuang HH, Lin S (2009). Oxidative challenges sensitize the capsaicin receptor by covalent cysteine modification. Proceedings of the National Academy of Sciences of the United States of America 106(47): 20097-20102.

Chung MK, Asgar J, Lee J, Shim MS, Dumler C, Ro JY (2015). The role of TRPM2 in hydrogen peroxide-induced expression of inflammatory cytokine and chemokine in rat trigeminal ganglia. Neuroscience 297: 160-169.

Corder G, Tawfik VL, Wang D, Sypek EI, Low SA, Dickinson JR, et al. (2017). Loss of mu opioid receptor signaling in nociceptors, but not microglia, abrogates morphine tolerance without disrupting analgesia. Nature medicine 23(2): 164-173.

Davis JB, Gray J, Gunthorpe MJ, Hatcher JP, Davey PT, Overend P, et al. (2000). Vanilloid receptor-1 is essential for inflammatory thermal hyperalgesia. Nature 405(6783): 183-187.

DelloStritto DJ, Connell PJ, Dick GM, Fancher IS, Klarich B, Fahmy JN, et al. (2016). Differential regulation of TRPV1 channels by H2O2: implications for diabetic microvascular dysfunction. Basic Research in Cardiology 111(2): 21.

Dickhout JG, Basseri S, Austin RC (2008). Macrophage Function and Its Impact on Atherosclerotic Lesion Composition, Progression, and Stability. Arteriosclerosis, Thrombosis, and Vascular Biology 28(8): 1413.

Dixon WJ (1980). Efficient analysis of experimental observations. Annual review of pharmacology and toxicology 20: 441-462.

Endres-Becker J, Heppenstall PA, Mousa SA, Labuz D, Oksche A, Schafer M, et al. (2007). Mu-opioid receptor activation modulates transient receptor potential vanilloid 1 (TRPV1) currents in sensory neurons in a model of inflammatory pain. Molecular Pharmacology 71(1): 12-18.

Erridge C, Kennedy S, Spickett CM, Webb DJ (2008). Oxidized Phospholipid Inhibition of Toll-like Receptor (TLR) Signaling Is Restricted to TLR2 and TLR4: ROLES FOR CD14, LPS-BINDING PROTEIN, AND MD2. The Journal of Biological Chemistry 283(36): 24748-24759.

Faria-Neto JR, Chyu KY, Li X, Dimayuga PC, Ferreira C, Yano J, et al. (2006). Passive immunization with monoclonal IgM antibodies against phosphorylcholine reduces accelerated vein graft atherosclerosis in apolipoprotein E-null mice. Atherosclerosis 189(1): 83-90.

Fernandes ES, Fernandes MA, Keeble JE (2012). The functions of TRPA1 and TRPV1: moving away from sensory nerves. British Journal of Pharmacology. 166.

Folch J, Lees M, Stanley GHS (1957). A SIMPLE METHOD FOR THE ISOLATION AND PURIFICATION OF TOTAL LIPIDES FROM ANIMAL TISSUES. Journal of Biological Chemistry 226(1): 497-509.

Friedman P, Horkko S, Steinberg D, Witztum JL, Dennis EA (2002a). Correlation of antiphospholipid antibody recognition with the structure of synthetic oxidized phospholipids. Importance of Schiff base formation and aldol condensation. The Journal of biological chemistry 277(9): 7010-7020.

Friedman P, Hörkkö S, Steinberg D, Witztum JL, Dennis EA (2002b). Correlation of Antiphospholipid Antibody Recognition with the Structure of Synthetic Oxidized Phospholipids: IMPORTANCE OF SCHIFF BASE FORMATION AND ALDOL CONDENSATION. Journal of Biological Chemistry 277(9): 7010-7020.

Frostegard J, Svenungsson E, Wu R, Gunnarsson I, Lundberg IE, Klareskog L, et al. (2005). Lipid peroxidation is enhanced in patients with systemic lupus erythematosus and is associated with arterial and renal disease manifestations. Arthritis and rheumatism 52(1): 192-200.

Fruhwirth GO, Loidl A, Hermetter A (2007) Oxidized phospholipids: from molecular properties to disease. Biochimica et Biophysica Acta 1772: 718–736.

Gabriel AF, Marcus MA, Honig WM, Walenkamp GH, Joosten EA. (2007). The CatWalk method: a detailed analysis of behavioral changes after acute inflammatory pain in the rat. Journal of Neuroscience Methods 163(1):9-16.

Gabriel AF, Marcus MA, Walenkamp GH, Joosten EA. (2009). The CatWalk method: Assessment of mechanical allodynia in experimental chronic pain. Behavioral Brain Research 198 (2009) 477–480

Gangadharan V, Kuner R (2013). Pain hypersensitivity mechanisms at a glance. Disease Models & Mechanisms 6(4): 889-895.

Getz GS, Wool GD, Reardon CA (2010). Biological Properties of Apolipoprotein A-I Mimetic Peptides. Current atherosclerosis reports 12(2): 96-104.

Hackel D, Krug SM, Sauer RS, Mousa SA, Bocker A, Pflucke D, et al. (2012). Transient opening of the perineurial barrier for analgesic drug delivery. Proceedings of the National Academy of Sciences of the United States of America 109(29): E2018-2027.

Hackel D, Pflucke D, Neumann A, Viebahn J, Mousa S, Wischmeyer E, et al. (2013). The connection of monocytes and reactive oxygen species in pain. PLoS One 8(5): e63564.

Haider L, Fischer MT, Frischer JM, Bauer J, Hoftberger R, Botond G, et al. (2011). Oxidative damage in multiple sclerosis lesions. Brain : a journal of neurology 134(Pt 7): 1914-1924.

Handa JT, Tagami M, Ebrahimi K, Leibundgut G, Janiak A, Witztum JL, et al. (2015). Lipoprotein(A) with An Intact Lysine Binding Site Protects the Retina From an Age-Related Macular Degeneration Phenotype in Mice (An American Ophthalmological Society Thesis). Transactions of the American Ophthalmological Society 113: T5.

Hargreaves K, Dubner R, Brown F, Flores C, Joris J (1988). A new and sensitive method for measuring thermal nociception in cutaneous hyperalgesia. Pain 32(1): 77-88.

Hörkkö S, Bird DA, Miller E, Itabe H, Leitinger N, Subbanagounder G, et al. (1999). Monoclonal autoantibodies specific for oxidized phospholipids or oxidized phospholipid–protein adducts inhibit macrophage uptake of oxidized low-density lipoproteins. Journal of Clinical Investigation 103(1): 117-128.

Huehnchen P, Boehmerle W, Endres M (2013). Assessment of Paclitaxel Induced Sensory Polyneuropathy with “Catwalk” Automated Gait Analysis in Mice. PLOS ONE 8(10): e76772.

Imai Y, Kuba K, Neely GG, Yaghubian-Malhami R, Perkmann T, van Loo G, et al. (2008). Identification of oxidative stress and Toll-like receptor 4 signaling as a key pathway of acute lung injury. Cell 133(2): 235-249.

Inoue K, Koizumi S, Fuziwara S, Denda S, Inoue K, Denda M (2002). Functional vanilloid receptors in cultured normal human epidermal keratinocytes. Biochemical and Biophysical Research Communications 291(1): 124-129.

Itabe H, Takeshima E, Iwasaki H, Kimura J, Yoshida Y, Imanaka T, et al. (1994). A monoclonal antibody against oxidized lipoprotein recognizes foam cells in atherosclerotic lesions. Complex formation of oxidized phosphatidylcholines and polypeptides. Journal of Biological Chemistry 269(21): 15274-15279.

Jain A, Bronneke S, Kolbe L, Stab F, Wenck H, Neufang G (2011). TRP-channel-specific cutaneous eicosanoid release patterns. Pain. 152.

Kaneko Y, Szallasi A (2014). Transient receptor potential (TRP) channels: a clinical perspective. British Journal of Pharmacology 171(10): 2474-2507.

Keeble JE, Bodkin JV, Liang L, Wodarski R, Davies M, Fernandes ES, et al. (2009). Hydrogen peroxide is a novel mediator of inflammatory hyperalgesia, acting via transient receptor potential vanilloid 1-dependent and independent mechanisms. Pain 141(1-2): 135-142.

Kochukov MY, McNearney TA, Fu Y, Westlund KN (2006). Thermosensitive TRP ion channels mediate cytosolic calcium response in human synoviocytes. American journal of physiology. Cell physiology 291(3): C424-432.

Koivisto A, Chapman H, Jalava N, Korjamo T, Saarnilehto M, Lindstedt K, et al. (2014). TRPA1: A Transducer and Amplifier of Pain and Inflammation. Basic & Clinical Pharmacology & Toxicology 114(1): 50-55.

Kwan KY, Allchorne AJ, Vollrath MA, Christensen AP, Zhang D-S, Woolf CJ, et al. (2006). TRPA1 Contributes to Cold, Mechanical, and Chemical Nociception but Is Not Essential for Hair-Cell Transduction. Neuron 50(2): 277-289.

Lee S, Birukov KG, Romanoski CE, Springstead JR, Lusis AJ, Berliner JA (2012). Role of Phospholipid Oxidation Products in Atherosclerosis. Circulation Research 111(6): 778-799.

Leitinger N (2008). The role of phospholipid oxidation products in inflammatory and autoimmune diseases: evidence from animal models and in humans. Sub-cellular biochemistry 49: 325-350.

Lennertz RC, Kossyreva EA, Smith AK, Stucky CL (2012). TRPA1 mediates mechanical sensitization in nociceptors during inflammation. PLoS One 7(8): e43597.

Leo S, D'Hooge R, Meert T (2010). Exploring the role of nociceptor-specific sodium channels in pain transmission using Nav1.8 and Nav1.9 knockout mice. Behavioural Brain Research 208(1): 149-157.

Li L, Hasan R, Zhang X (2014). The basal thermal sensitivity of the TRPV1 ion channel is determined by PKCβII. Journal of Neuroscience 34(24): 8246-58.

Liu B, Tai Y, Caceres AI, Achanta S, Balakrishna S, Shao X, et al. (2016). Oxidized Phospholipid OxPAPC Activates TRPA1 and Contributes to Chronic Inflammatory Pain in Mice. PLoS ONE 11(11): e0165200.

Martin C, Stoffer C, Mohammadi M, Hugo J, Leipold E, Oehler B, Rittner HL, Blum R. (2018) NaV1. 9 Potentiates Oxidized Phospholipid-Induced TRP Responses Only under Inflammatory Conditions. Frontiers in Molecular Neuroscience 11, 7

Masmoudi H, Mota-Santos T, Huetz F, Coutinho A, Cazenave PA (1990). All T15 Id-positive antibodies (but not the majority of VHT15+ antibodies) are produced by peritoneal CD5+ B lymphocytes. International immunology 2(6): 515-520.

Matt U, Sharif O, Martins R, Furtner T, Langeberg L, Gawish R, et al. (2013). WAVE1 mediates suppression of phagocytosis by phospholipid-derived DAMPs. The Journal of clinical investigation 123(7): 3014-3024.

Mittal M, Siddiqui MR, Tran K, Reddy SP, Malik AB (2014). Reactive oxygen species in inflammation and tissue injury. Antioxidants & Redox Signaling 20(7): 1126-1167.

Miyake T, Nakamura S, Zhao M, So K, Inoue K, Numata T, et al. (2016). Cold sensitivity of TRPA1 is unveiled by the prolyl hydroxylation blockade-induced sensitization to ROS. Nature Communications 7: 12840.

Mogil JS (2009). Animal models of pain: progress and challenges. Nature Reviews Neuroscience Journal 10(4): 283-294.

Mogil, JS, Graham, AC, Ritchie, J. (2010). Hypolocomotion, asymmetrically directed behaviors (licking, lifting, flinching, and shaking) and dynamic weight bearing (gait) changes are not measures of neuropathic pain in mice. Molecular Pain 6: 34.

Mohammadi M, Oehler B, Kloka J, Martin C, Brack A, Blum R, Rittner HL. (2018). Antinociception by the anti-oxidized phospholipid antibody E06. British journal of pharmacology 175(14)

Mohammadi M, Bergado-Acosta JR, Fendt M. (2014) Relief learning is distinguished from safety learning by the requirement of the nucleus accumbens. Behavioural brain research 272, 40-45

Mohammadi M, Fendt M. (2015) Relief learning is dependent on NMDA receptor activation in the nucleus accumbens. British journal of pharmacology 172 (9), 2419-2426

Nandedkar SD, Weihrauch D, Xu H, Shi Y, Feroah T, Hutchins W, et al. (2011). D-4F, an apoA-1 mimetic, decreases airway hyperresponsiveness, inflammation, and oxidative stress in a murine model of asthma. Journal of Lipid Research 52(3): 499-508.

Naylor J, Al-Shawaf E, McKeown L, Manna PT, Porter KE, O'Regan D, et al. (2011). TRPC5 channel sensitivities to antioxidants and hydroxylated stilbenes. The Journal of biological chemistry 286(7): 5078-5086.

Nicholas S, Yuan SY, Brookes SJ, Spencer NJ, Zagorodnyuk VP (2017). Hydrogen peroxide preferentially activates capsaicin-sensitive high threshold afferents via TRPA1 channels in the guinea pig bladder. British Journal of Pharmacology 174(2): 126-138.

Nilius B, Appendino G, Owsianik G (2012). The transient receptor potential channel TRPA1: from gene to pathophysiology. Pflugers Arch. 464.

Nummenmaa E, Hämäläinen M, Moilanen LJ, Paukkeri E-L, Nieminen RM, Moilanen T, et al. (2016). Transient receptor potential ankyrin 1 (TRPA1) is functionally expressed in primary human osteoarthritic chondrocytes. Arthritis Research & Therapy 18(1): 185.

Oehler B, Kistner K, Martin C, Schiller J, Mayer R, Mohammadi M, et al. (2017a). Inflammatory pain control by blocking oxidized phospholipid-mediated TRP channel activation. Scientific reports 7(1): 5447.

Oehler, B., Mohammadi, M., Perpina Viciano, C., Hackel, D., Hoffmann, C., Brack, A., and Rittner, H.L. (2017b). Peripheral Interaction of resolvin D1 and E1 with opioid receptor antagonists for antinociception in inflammatory pain in rats. Frontiers in molecular neuroscience10, 242.

Ogawa N, Kurokawa T, Fujiwara K, Polat OK, Badr H, Takahashi N, et al. (2016a). Functional and Structural Divergence in Human TRPV1 Channel Subunits by Oxidative Cysteine Modification. Journal of Biological Chemistry 291(8): 4197-4210.

Ogawa N, Kurokawa T, Mori Y (2016b). Sensing of redox status by TRP channels. Cell Calcium 60(2): 115-122.

Östman JAR, Nassar MA, Wood JN, Baker MD (2008). GTP up-regulated persistent Na(+) current and enhanced nociceptor excitability require Na(V)1.9. The Journal of physiology 586(Pt 4): 1077-1087.

Palinski W, Horkko S, Miller E, Steinbrecher UP, Powell HC, Curtiss LK, et al. (1996). Cloning of monoclonal autoantibodies to epitopes of oxidized lipoproteins from apolipoprotein E-deficient mice.

Demonstration of epitopes of oxidized low density lipoprotein in human plasma. The Journal of clinical investigation 98(3): 800-814.

Patwardhan AM, Akopian AN, Ruparel NB, Diogenes A, Weintraub ST, Uhlson C, et al. (2010). Heat generates oxidized linoleic acid metabolites that activate TRPV1 and produce pain in rodents. The Journal of clinical investigation 120(5): 1617-1626.

Paulsen CE, Armache J-P, Gao Y, Cheng Y, Julius D (2015). Structure of the TRPA1 ion channel suggests regulatory mechanisms. Nature 520(7548): 511-517.

Pereira I, Mendes SJ, Pereira DM, Muniz TF, Colares VL, Monteiro CR, et al. (2017). Transient Receptor Potential Ankyrin 1 Channel Expression on Peripheral Blood Leukocytes from Rheumatoid Arthritic Patients and Correlation with Pain and Disability. Frontiers in pharmacology 8: 53.

Pflucke D, Hackel D, Mousa SA, Partheil A, Neumann A, Brack A, et al. (2013). The molecular link between C-C-chemokine ligand 2-induced leukocyte recruitment and hyperalgesia. The journal of pain: official journal of the American Pain Society 14(9): 897-910.

Pitzer C, Kuner R, Tappe-Theodor A. (2016). Voluntary and evoked behavioral correlates in inflammatory pain conditions under different social housing conditions. Pain Reports Aug 9; 1(1):e564

Qin J, Goswami R, Balabanov R, Dawson G (2007). Oxidized phosphatidylcholine is a marker for neuroinflammation in multiple sclerosis brain. Journal of neuroscience research 85(5): 977-984.

Que X, Hung MY, Yeang C, Gonen A, Prohaska TA, Sun X, Diehl C, Määttä A, Gaddis DE, Bowden K, Pattison J, MacDonald JG, Ylä-Herttuala S, Mellon PL, Hedrick CC, Ley K6, Miller YI, Glass CK, Peterson KL, Binder CJ, Tsimikas S, Witztum JL. (2018) Oxidized phospholipids are proinflammatory and proatherogenic in hypercholesterolaemic mice. Nature 558(7709):301-306

Randall LO, Selitto JJ (1957). A method for measurement of analgesic activity on inflamed tissue. Archives internationales de pharmacodynamie et de therapie 111(4): 409-419.

Ravandi A, Leibundgut G, Hung MY, Patel M, Hutchins PM, Murphy RC, et al. (2014). Release and capture of bioactive oxidized phospholipids and oxidized cholesteryl esters during percutaneous coronary and peripheral arterial interventions in humans. Journal of the American College of Cardiology 63(19): 1961-1971.

Rittner HL, Hackel D, Voigt P, Mousa S, Stolz A, Labuz D, et al. (2009). Mycobacteria Attenuate Nociceptive Responses by Formyl Peptide Receptor Triggered Opioid Peptide Release from Neutrophils. PLOS Pathogens 5(4): e1000362.

Seimon T, Tabas I (2009). Mechanisms and consequences of macrophage apoptosis in atherosclerosis. Journal of Lipid Research 50(Suppl): S382-S387.

Seimon TA, Nadolski MJ, Liao X, Magallon J, Nguyen M, Feric NT, et al. (2010). Atherogenic Lipids and Lipoproteins Trigger CD36-TLR2-Dependent Apoptosis in Macrophages Undergoing Endoplasmic Reticulum Stress. Cell metabolism 12(5): 467-482.

Shaw PX, Horkko S, Chang MK, Curtiss LK, Palinski W, Silverman GJ, et al. (2000). Natural antibodies with the T15 idiotype may act in atherosclerosis, apoptotic clearance, and protective immunity. Journal of Clinical Investigation 105(12): 1731-1740.

Somogyi CS, Matta C, Foldvari Z, Juhasz T, Katona E, Takacs AR, et al. (2015). Polymodal Transient Receptor Potential Vanilloid (TRPV) Ion Channels in Chondrogenic Cells. International journal of molecular sciences 16(8): 18412-18438.

Stucky CL, Dubin AE, Jeske NA, Malin SA, McKemy DD, Story GM (2009). Roles of transient receptor potential channels in pain. Brain Research Reviews 60(1): 2-23.

Sugiyama D, Kang S, Brennan TJ (2017). Muscle Reactive Oxygen Species (ROS) Contribute to Post-Incisional Guarding via the TRPA1 Receptor. PLoS One 12(1): e0170410.

Sumoza-Toledo A, Penner R (2011). TRPM2: a multifunctional ion channel for calcium signalling. The Journal of Physiology. 589(7):1515-25.

Tan CH, McNaughton PA (2016). The TRPM2 ion channel is required for sensitivity to warmth. Nature 536(7617): 460-463.

Tappe-Theodor A, Kuner R (2014). Studying ongoing and spontaneous pain in rodents – challenges and opportunities. European Journal of Neuroscience 39(11): 1881-1890.

Thayaparan D, Shen P, Stampfli MR, Morissette MC (2016). Induction of pulmonary antibodies against oxidized lipids in mice exposed to cigarette smoke. Respiratory Research 17(1): 97.

Thimmulappa RK, Gang X, Kim JH, Sussan TE, Witztum JL, Biswal S (2012). Oxidized phospholipids impair pulmonary antibacterial defenses: evidence in mice exposed to cigarette smoke. Biochemical and Biophysical Research Communications 426(2): 253-259.

Trevisan G, Benemei S, Materazzi S, De Logu F, De Siena G, Fusi C, et al. (2016). TRPA1 mediates trigeminal neuropathic pain in mice downstream of monocytes/macrophages and oxidative stress. Brain: a journal of neurology 139(Pt 5): 1361-1377.

Trevisan G, Hoffmeister C, Rossato MF, Oliveira SM, Silva MA, Ineu RP, et al. (2013b). Transient Receptor Potential Ankyrin 1 Receptor Stimulation by Hydrogen Peroxide Is Critical to Trigger Pain During Monosodium Urate–Induced Inflammation in Rodents. Arthritis & Rheumatism 65(11): 2984-2995.

Trevisani M, Siemens J, Materazzi S, Bautista DM, Nassini R, Campi B, et al. (2007a). 4-Hydroxynonenal, an endogenous aldehyde, causes pain and neurogenic inflammation through activation of the irritant receptor TRPA1. Proceedings of the National Academy of Sciences of the United States of America 104(33): 13519-13524.

Tsiantoulas D, Gruber S, Binder CJ (2012). B-1 Cell Immunoglobulin Directed Against Oxidation-Specific Epitopes. Frontiers in Immunology 3: 415.

Usui K, Hulleman JD, Paulsson JF, Siegel SJ, Powers ET, Kelly JW (2009). Site-specific modification of Alzheimer's peptides by cholesterol oxidation products enhances aggregation energetics and neurotoxicity. Proceedings of the National Academy of Sciences of the United States of America 106(44): 18563-18568.

Vandewauw I, De Clercq K, Mulier M, Held K, Pinto S, Van Ranst N, Segal A, Voet T, Vennekens R, Zimmermann K, Vriens J, Voets T (2018). A TRP channel trio mediates acute noxious heat sensing. Nature. 555(7698):662-666.

Van Lenten BJ, Wagner AC, Jung CL, Ruchala P, Waring AJ, Lehrer RI, et al. (2008). Anti-inflammatory apoA-I-mimetic peptides bind oxidized lipids with much higher affinity than human apoA-I. The Journal of Lipid Research 49(11): 2302-2311.

Vay, L., Gu, C., & McNaughton, P. A. (2012). The thermo-TRP ion channel family: properties and therapeutic implications. British Journal of Pharmacology, 165(4), 787-801. doi:10.1111/j.1476-5381.2011.01601.x

Viana F (2016). TRPA1 channels: molecular sentinels of cellular stress and tissue damage. The Journal of physiology 594(15): 4151-4169.

Watson AD, Leitinger N, Navab M, Faull KF, Horkko S, Witztum JL, et al. (1997). Structural identification by mass spectrometry of oxidized phospholipids in minimally oxidized low density lipoprotein that induce monocyte/endothelial interactions and evidence for their presence in vivo. Journal of Biological Chemistry 272(21): 13597-13607.

Yun MR, Park HM, Seo KW, Lee SJ, Im DS, Kim CD (2010). 5-Lipoxygenase plays an essential role in 4-HNE-enhanced ROS production in murine macrophages via activation of NADPH oxidase. Free Radical Research 44(7): 742-750.

Zappia KJ, O'Hara CL, Moehring F, Kwan KY, Stucky CL (2017). Sensory neuron-specific deletion of TRPA1 results in mechanical cutaneous sensory deficits. eneuro.

Zhang X (2015). Molecular sensors and modulators of thermoreception. Channels (Austin) 9(2): 73-81.